Division of Applied Sciences
Harvard University — Cambridge, Massachusetts

ANNUAL PROGRESS REPORT NO. 103

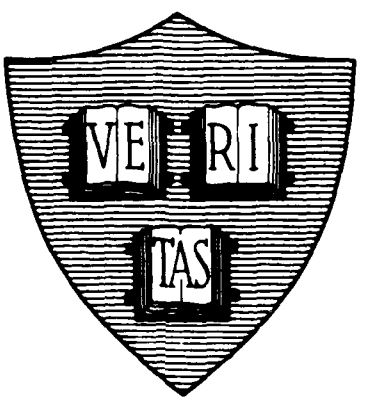

JOINT SERVICES ELECTRONICS PROGRAM
N00014–89–J–1023

Covering Period

October 1, 1988 — July 31, 1989

July 1989

REPORT DOCUMENTATION PAGE

Form Approved
OMB No 0704 0188
Exp Date Jun 30 1986

1a REPORT SECURITY CLASSIFICATION Unclassified	1b RESTRICTIVE MARKINGS None
2a SECURITY CLASSIFICATION AUTHORITY N/A	3 DISTRIBUTION/AVAILABILITY OF REPORT Unclassified/Unlimited
2b DECLASSIFICATION/DOWNGRADING SCHEDULE N/A	
4 PERFORMING ORGANIZATION REPORT NUMBER(S) Annual Progress Report No. 103	5 MONITORING ORGANIZATION REPORT NUMBER(S)
6a NAME OF PERFORMING ORGANIZATION Harvard University	6b OFFICE SYMBOL (If applicable) N/A
6c. ADDRESS (City, State, and ZIP Code) Division of Applied Sciences Harvard University Cambridge, MA 02138	7a NAME OF MONITORING ORGANIZATION Office of Naval Research 7b ADDRESS (City, State, and ZIP Code) 800 N. Quincy Street Arlington, VA 22217
8a. NAME OF FUNDING/SPONSORING ORGANIZATION Office of Naval Research	8b OFFICE SYMBOL (If applicable)
8c. ADDRESS (City, State, and ZIP Code) 800 N. Quincy Street Arlington, VA 22217	9 PROCUREMENT INSTRUMENT IDENTIFICATION NUMBER N00014-89-J-1023 10 SOURCE OF FUNDING NUMBERS

PROGRAM ELEMENT NO	PROJECT NO	TASK NO	WORK UNIT ACCESSION NO

11. TITLE (Include Security Classification)
Annual Progress Report No. 103

12 PERSONAL AUTHOR(S)
Prof. Michael Tinkham

13a. TYPE OF REPORT	13b TIME COVERED	14 DATE OF REPORT (Year, Month, Day)	15 PAGE COUNT
Technical	FROM 10/1/88 TO 7/31/89	July 31, 1989	104

16. SUPPLEMENTARY NOTATION

17 COSATI CODES			18. SUBJECT TERMS (Continue on reverse if necessary and identify by block number)
FIELD	GROUP	SUB-GROUP	

19. ABSTRACT (Continue on reverse if necessary and identify by block number)

An annual report of the JSEP (Joint Services Electronics Program) in solid state electronics, quantum electronics, information electronics, control and optimization, and electromagnetic phenomena is presented. Results of the research to date are summarized and significant accomplishments are discussed.

20 DISTRIBUTION/AVAILABILITY OF ABSTRACT ☐ UNCLASSIFIED/UNLIMITED ☐ SAME AS RPT ☐ DTIC USERS	21 ABSTRACT SECURITY CLASSIFICATION Unclassified
22a NAME OF RESPONSIBLE INDIVIDUAL	22b TELEPHONE (Include Area Code) / 22c OFFICE SYMBOL

DD FORM 1473, 84 MAR — 83 APR edition may be used until exhausted. All other editions are obsolete.

SECURITY CLASSIFICATION OF THIS PAGE

Joint Services Electronics Program

N00014-89-J-1023

ANNUAL PROGRESS REPORT NO. 103

Covering Period

October 1, 1988 — July 31, 1989

The research reported in this document, unless otherwise indicated, was made possible through support extended to the Division of Applied Sciences, Harvard University by the U. S. Army Research Office, the U. S. Air Force Office of Scientific Research and the U. S. Office of Naval Research under the Joint Services Electronics Program by Grant N00014-89-J-1023. Related research sponsored by the Office of Naval Research, the National Science Foundation, the National Aeronautic and Space Administration, and by the University is also reported briefly with appropriate acknowledgment.

Division of Applied Sciences
Harvard University
Cambridge, Massachusetts

ANNUAL PROGRESS REPORT NO. 103

Joint Services Contract

N00014–89–J–1023	The Steering Committee

Related Contracts

N00014–86–K–0033	H. Ehrenreich
N00014–86–K–0075	Y. C. Ho
N00014–86–K–0744	W. Paul
N00014–86–K–0760	H. Ehrenreich
N00014–86–K–0841	H. Ehrenreich
N00014–89–J–1565	M. Tinkham
NSF-ECS–85–15449	Y. C. Ho
NSF-CDR–85–00108	Y. C. Ho
NSF-DMR–84–04489	M. Tinkham
NSF-DMR–85–03896	Y. C. Ho
NSF-DMR–86–14003	W. Paul, P. S. Pershan, M. Tinkham, R. M. Westervelt
NSF-DMR–88–12855	P. S. Pershan
NSF-DMR–88–58075	N. Bloembergen, E. Mazur
NSF-FCS–86–58157	Y. C. Ho
DAAG29–85–K–0060	E. Mazur
DAAL02–86–K–0095	T. T. Wu
DAAL03–88–K–0114	E. Mazur
DE-FG02–84–ER40158	T. T. Wu
DE-FG02–88–ER45379	P. S. Pershan
F19628–88–K–0024	T. T. Wu

JOINT SERVICES ELECTRONICS PROGRAM

October 1, 1988 — July 31, 1989

ADMINISTRATIVE STAFF

Contracts

N00014–89–J–1023

The Steering Committee

Prof. N. Bloembergen
Asst. Prof. J. J. Clark
Prof. H. Ehrenreich
Prof. J. A. Golovchenko
Prof. Y. C. Ho
Assoc. Prof. E. Mazur
Prof. W. Paul
Prof. P. S. Pershan
Prof. M. Tinkham
Prof. R. M. Westervelt
Prof. T. T. Wu
Assoc. Prof. D. D. Yao
Dr. P. McKinney

RESEARCH STAFF

Dr. N. Bloembergen
Dr. M. Buijs
Dr. J. J. Clark
Dr. H. Ehrenreich
Dr. Y. C. Ho
Dr. N. F. Johnson
Dr. R. W. P. King
Dr. C. J. Lobb
Dr. E. Mazur
Dr. J. M. Myers
Dr. W. Paul
Dr. P. S. Pershan
Dr. T. Rabedeau
Dr. M. Rzchowski
Dr. H.-M. Shen
Dr. S. Strickland
Dr. P. Q. Tang
Dr. M. Tinkham
Dr. Dr. R. M. Westervelt
Dr. T. T. Wu
Dr. D. D. Yao
Dr. J. Zhang

INTRODUCTION

This report covers progress made during the past year in the work of eleven Research Units funded under the Joint Services Electronics Program at Harvard University. It is broken down into four major divisions of electronic research: *Solid state electronics, Quantum electronics, Information electronics, and Electromagnetic phenomena.* Following the report of the work of each Unit, there is a complete annual report of the associated Publications/Patents/Presentations/Honors. This report also includes a section on *Significant Accomplishments* which contains selected highlights from two of these areas. These are "Harmonic Generation in High-Temperature Superconductors" by Research Unit 4 and "Resonant Closed Loops of Dipoles" by Research Unit 11.

CONTENTS

V. SIGNIFICANT ACCOMPLISHMENTS REPORT

I. SOLID STATE ELECTRONICS

Personnel

Prof. H. Ehrenreich
Prof. W. Paul
Prof. P. S. Pershan
Prof. M. Tinkham
Prof. R. M. Westervelt
Assoc. Prof. C. J. Lobb
Dr. M. Iansiti
Dr. N. F. Johnson
Dr. T. Rabedeau
Dr. M. Rzchowski

Mr. Mr. K. Babcock
Mr. S. P. Benz
Mr. J. H. Burnett
Mr. H. Cheong
Mr. L. Ji
Mr. A. T. Johnson
Mr. C. M. Marcus
Mr. R. Martinez
Mr. I. Tidswell
Mr. F. Waugh

I.1 Electronic Theory of Semiconductor Alloys and Superlattices. H. Ehrenreich, Grant N00014–89–J–1023; Research Unit 1.

During the past year the efforts of the group have been concentrated mainly on the electronic and optical properties of superlattices and the electronic and magnetic properties of diluted magnetic semiconductors.

A. Superlattices

Superlattices are assuming increasing importance in both optoelectronic and infrared detector applications. We have developed a superlattice representation formalism, based on a $\mathbf{k} \cdot \mathbf{p}$ approach, which is optimally adapted to calculating electronic structure and the optical properties of superlattices using an extended Kane model and the associated parameters for the bulk as the only input. Applications to the band structure and optical properties of superlattices have been shown to be in quantitative agreement with both experiment and the results of other, more elaborate calculational schemes.

HgTe/CdTe superlattices has been resolved [2]. We have shown that the effective mass and the band gap obtained in the magnetooptical experiments are consistent with the larger value of the valence band offset. This is due to the fact that the conduction and valence bands of the semiconductor superlattices cross as the offset is increased from small values and render the materials semimetallic. What had been missed is the fact that the superlattice again becomes semiconducting as the offset is increased further. This resolution of the dilemma is appealing because it recognizes that both magneto-optical and photoemission experimental results are consistent with each other and simply notes that there has been an oversight on the part of theorists in failing to recognize that after the semimetallic regime, the superlattice band structure becomes once again semiconducting with the band gap at the superlattice Brillouin zone. These results have been published in *Phys. Rev. Lett.* [1,2].

References:

1. N. F. Johnson, H. Ehrenreich and R. V. Jones, "Carrier-Activated Light Modulation," *Phys. Rev. Lett.* **53**(3), 180 (1988).

2. N. F. Johnson, P. M. Hui and H. Ehrenreich, "Valence Band Offset Controversy in HgTe/CdTe Superlattices: A Possible Resolution," *Phys. Rev. Lett.* **61**(17), 1993 (1988).

B. Magnetic Properties of Diluted Magnetic Semiconductors

The investigations of magnetic disorder in DMS have led to an empirically based and internally consistent picture of the electronic structure of these materials. This picture is consistent with the existing experimental information, and, to the best of our knowledge, inconsistent with none. It has been used to describe the magnetic interactions in the Mn-alloyed II-VI DMS on a microscopic basis. As a result, it has been possible to develop a description of the electronic and magnetic interactions on energy scales ranging from 10^{-5} eV to 10 eV.

We have considered compounds of the form $(II)_{1-x}Mn_x(VI)$ for a variety of ingredients belonging to Groups II (Hg,Cd,Zn) and VI (Te,Se,S) of the periodic table.

We have examined both isotropic and anisotropic exchange for CdMnTe and related materials. In the case of the isotropic exchange these represent the most accurate available results thus far for any magnetic insulator. The reason for this improvement is associated with better knowledge of the electronic structure for semiconductors and the utilization of the empirically determined Te p - Mn d exchange interactions.

During the past year we have published [1] a quantitative calculation of isotropic superexchange and an explanation of the spin resonance linewidth narrowing in diluted magnetic semiconductors. The Dzyaloshinski-Moriya anisotropic superexchange is the dominant mechanism determining the paramagnetic resonance (EPR) linewidth in Mn-based II-VI DMS such as $Cd_{1-x}Mn_xTe$. The Anderson Hamiltonian which was applied in our previous study of isotropic superexchange has been generalized to include the anion spin-orbit coupling responsible for anisotropic superexchange. The EPR lineshape has been calculated using a moment expansion of the magnetic response function to first order in inverse temperature together with a maximum entropy ansatz. The calculated infinite temperature linewidths are in good agreement with extrapolated experimental values obtained by Samarth and Furdyna. A novel fit of the theoretical temperature dependence to the experimental linewidth data provides the first empirical value for the anisotropic exchange constant. This value is in excellent agreement with that obtained by our theoretical calculation. The calculated chemical trends for the exchange constants for the selenides and sulfides yield the experimentally expected trends.

Reference:

1. B. E. Larson and H. Ehrenreich, "Anisotropic Exchange and EPR Linewidths in Dilluted Magnetic Semiconductors", *Phys. Rev. B.* **39**(3), 1747 (1989).

ANNUAL REPORT OF

PUBLICATIONS/PATENTS/PRESENTATIONS/HONORS

a. Papers Submitted to Refereed Journals (and not yet published)

N. F. Johnson and H. Ehrenreich, "Infrared Optical Properties of III–V and II–VI Superlattices," submitted to *Surface Science*. (Partially supported by N00014–86–K–0465, N00014–89–J–1023 and N00014–86–K–0033)

P. M. Hui, H. Ehrenreich, and K. C. Hass, "Effects of *d* Bands on Semiconductor *sp* Hamiltonians, submitted to *Phys. Rev.* **B**. (Partially supported by N00014–86–K–0760)

N. F. Johnson, H. Ehrenreich, P. M. Hui, and P. M. Young, "Electronic and Optical Properties of III–V and II–VI Semiconductor Superlattices," *Phys. Rev. Lett.* **B**. (Partially supported by N00014–86–K–0033)

b. Papers Published in Refereed Journals

N. F. Johnson, P. M. Hui, and H. Ehrenreich, "Valence-Band-Offset Controversy in HgTe/CdTe Superlattices: A Possible Resolution," *Phys. Rev. Lett.* **61**, 1993 (1988). (Partially supported by N00014–86–K–0033, N00014–86–K–0465)

N. F. Johnson, H. Ehrenreich, G. Y. Wu, and T. C. McGill, "Superlattice $k \cdot p$ Models for Calculating Electronic Structure," *Phys. Rev.* **B39** (13), 95 (1988). (Partially supported by N00014–86–K–0465, N00014–86–K–0033, N00014–86–K–0760, N00014–86–K–0841)

B. E. Larson and H. Ehrenreich, "Anisotropic Superexchange and Spin-Resonance Linewidth in Diluted Magnetic Semiconductors," *Phys. Rev.* **B39**, 1747 (1989). (Partially supported by N00014–86–K–0760)

P. M. Hui, H. Ehrenreich and N. F. Johnson, "A Possible Resolution of the Valence-Band Offset Controversy in HgTe/CdTe Superlattices," *J. Vac. Sci. Technol.* **A7**, 424 (1989). (Partially supported by N00014–86–K–0033, N00014–86–K–0465)

c. Books (and sections thereof) Submitted for Publication

Editor (with D. Turnbull), *Solid State Physics*, Vol. 43 (Academic Press, 1990).

d. Books (and sections thereof) Published

Editor (with D. Turnbull), *Solid State Physics*, Vol. 42 (Academic Press, 1989).

I.2 Pressure Dependence of Photo-Luminescence Excitation in GaAs/$Al_xGa_{1-x}As$ Multi-Quantum Wells.

J. H. Burnett, H. M. Cheong, and W. Paul, Grants N00014–89–J–1023 and N00014–86–K-0744; Research Unit 2.

We have continued our work on the properties of multi-quantum-wells and superlattices of the group 3–group 5 compounds such as GaAs and $Ga_{1-x}Al_xAs$. Our particular approach is to study the pressure dependence of suitable optical spectra of such structures as a way to clarify the mechanisms of quantized state formation and of tunneling between adjacent wells. The rationale for this method is the fact that the pressure dependences of the band structures of the well and barrier material are well established, and therefore a pressure experiment may be used to study the effect of varying the band structures in a known way in a single structure, without courting the difficulty of unknown parameter changes when materials of different x-value, or different dimensions, are made.

The optical spectra chosen as the most suitable for high-pressure experimentation are the photoluminescence (PL) and photoluminescence excitation (PLE) spectra of GaAs wells between $Ga_{1-x}Al_xAs$ barriers. For $x = 0.3$, and for pressures below 40 kbar, the principal effect of pressure is to alter the nature of the barrier: the Γ minima, which are the lower at atmospheric pressure, become higher than the X minima for pressures greater than about 10 kbar. The coupling between wells (in a suitably-designed structure) is expected to depend on the relative energies of the barrier Γ and X states. Thus the experiments involve a detailed study of the changes in the spectra, and of the energies of the coupled states deduced from them, especially in the pressure range between 10 and 40 kbar.

We have designed GaAs/$Ga_{1-x}Al_xAs$ structures with different degrees of coupling between pairs of wells at atmospheric pressure. These have been fabricated in collaboration with E. Koteles and B. Elman of GTE Laboratories.

In our last report we described measurements, using PL and PLE, of electron

energy states as a function of pressure for strongly-coupled double quantum wells (CDQW). These were chosen as structures whose electron states would be expected to be especially affected by $\Gamma - X$ band mixing as the X band is driven through the barrier between the two wells by pressure. For a CDQW the electron energy levels are split into doublets, and the size of the doublet splitting, Δe, is a measure of the coupling between the wells. Admixture of X band states to the predominantly Γ-like wavefunctions tunneling through the barrier region would affect the nature of the wavefunctions, and thus the coupling between the wells, and hence the doublet splitting Δe. Also the energy of the electron states above the bulk conduction band minimum of the well material at a given pressure is a measure of the confinement of the electron states. Coupling of the electron states of the two wells delocalizes the electrons and lowers the confinement energy, E_c. Thus, any $\Gamma - X$ mixing should affect E_c as well.

We have previously reported preliminary results that E_c and Δe show anomalous behavior at and above the pressure region where the X band of the barrier crosses the electron levels. This behavior could not be explained as resulting from a pressure-dependent effective mass, m^*, and we suggested that this was evidence for $\Gamma - X$ mixing. However, simple models of band mixing of bulk states of different symmetry have not been able to explain our results quantitatively, and more rigorous models have yet to be established and accepted. This is in part due to a lack of consensus on the appropriate boundary conditions for envelope function calculations in the case of heterojunctions of semiconductors of different conduction band minima symmetry, and indeed whether envelope function models are adequate at all in this case. We believe that our results provide a good test for the appropriate band structure model in these circumstances. We have begun, in collaboration with band structure theorists, a program on this front.

However, our primary emphasis has been to confirm and elaborate these results

on other samples. Of particular emphasis has been developing techniques aimed at eliminating possible spurious components of our measurements that could undermine the conclusions. The main possible objection to our results is the possibility that the electron energy levels that we measured were affected by nonhydrostatic stress components. The samples were unmounted and in fact moved between pressure measurements to insure that there was no strain on the samples due to the pressure cell walls.

More difficult is the problem of nonhydrostatic pressure components of the pressure medium. There is as yet no published work quantitatively evaluating the nonhydrostaticity of various pressure media at low temperatures, though it is often stated that Ar is a good cryostatic pressure medium. We found that this "cryostatic medium" substantially broadens our PLE peaks, and hence complicates their quantitative interpretation. It offers no improvement over the methanol/ethanol mixture used in our initial measurements. We therefore had to do an investigation of various pressure media for their properties at low temperature, concentrating on those that are reported to be good at high pressure and room temperature: Methanol/Ethanol, Ar, N_2, Xe, and He.

We found that only He was hydrostatic enough at low temperatures for our purposes. In fact we observed no PL or PLE line broadening (to within 3%) at 4.6 K for pressures up to 40 kbars. The high compressibility of solid He (a factor of 3 in volume from .2 to 30 kbars), in part responsible for its good properties as a low temperature pressure medium, gives rise to certain technical difficulties, but its use eliminates any questions of spurious stresses [1].

We have proceeded to use these techniques on similar measurements of other CDQW samples. We have found that all our previous conclusions on the behavior of E_c and Δe are confirmed qualitatively, but with experimental uncertainty considerably reduced. At and above the pressure at which the X band of the barrier separating the

two wells crosses the lowest electron levels, E_c and Δe drop in energy by an amount dependent on the parameters of the CDQW. We feel that these results contain a quantitative measure of $\Gamma - X$ mixing and that any band mixing model must be consistent with these results. We are now proceeding on a program to put more sophisticated models to this test.

Reference:

1. J. H. Burnett and H. M. Cheong, "The Rare Gases Xe, Ar, and He as Cryogenic Pressure Media," submitted to *Rev. Sci. Instrum.*

ANNUAL REPORT OF

PUBLICATIONS/PATENTS/PRESENTATIONS/HONORS

a. Papers Submitted to Refereed Journals (and not yet published)

J. H. Burnett, H. M. Cheong, W. Paul, E. S. Koteles, and B. Elman, "Modification of the Coupling of Double Quantum Wells Through Band Structure Changes under Hydrostatic Pressure," to be published in the (refereed) Proceedings of the 4th International Conference on Superlattices, Microstructures, and Microdevices, Trieste, 1988.

J. H. Burnett and H. M. Cheong, "The Rare Gases Xe, Ar, and He as Cryogenic Pressure Media," submitted to *Rev. Sci. Instrum.*

g. Invited Presentations at Topical or Scientific/Technical Society Conferences

W. Paul, Lectures on "Phototransport Process" at the University N. Copernicus, Torun, Poland, at the University of Campinas, Brazil, and at a Summer School, Oran, Algeria, Summer 1988.

W. Paul, Invited Inaugural Presentation at an International Conference on "Narrow Gap Semiconductors," Gaithersburg, Maryland, June 1989.

j. Graduate Students and Postdoctorals Supported Under the JSEP for the Year Ending July 31, 1989.

Mr. J. H. Burnett and Mr. H. Cheong.

I.3 X-Ray Surface Characterization. I. Tidswell, T. Rabedeau and P. S. Pershan, Grants N00014–89–J-1023, NSF DMR–85–13523, and NSF DMR–86–14003; Research Unit 3.

The design and function of many modern electronic devices is critically dependent on the properties of surfaces. To this end major research efforts at many industrial and governmental laboratories have been directed towards developing new, and improved, techniques for characterization of solid surfaces [1]. These include electron diffraction and electron microscopy, as well as newer techniques such as tunneling electron microscopy and ion beam diffraction. On the other hand there are no comparable techniques capable of characterizing the structure buried interfaces [2]. In addition none of the above mentioned techniques provide a complete description of the surface structure of solids and other complementary techniques are needed. We have demonstrated that specular reflection of X-rays with energies in the range of 7 keV to 15 keV can be used to characterize the surface structure of simple liquids, liquid crystals, and solids and we propose continued development of the technique and application of the technique to surface problems relevant to electronics [3–10].

In particular if θ defines the angle of incidence as measured from the grazing condition (*i.e.*, $\theta = 90°$ is normal incidence) then the ratio between the reflected intensity $R(\theta)$ and the theoretical Fresnel Reflection Law of classical optics, $R_F(\theta)$, for a sharp flat surface with no structure is given by the relation:

$$\frac{R(\theta)}{R_F(\theta)} = \left| \rho_\infty^{-1} \int dz \left\langle \frac{\partial \rho}{\partial z} \right\rangle \exp\left[-iQz\right] \right|^2$$

where ρ_∞ is the electron density far from the surface, $Q = (4\pi/\lambda)\sin(\theta)$ and $R_F(\theta) \approx (\theta_c/2\theta)^4$ when $\theta >> \theta_c$. For X-rays in the range of 10 keV the dielectric constant for many materials is approximately given by the form $\epsilon \approx 1 - \rho_\infty r_e \lambda^2/\pi$ and the "critical angle" $\theta_c \approx \sqrt{1-\epsilon}$ is typically of the order of 0.2° to 0.3° [11]. For a rough, or diffuse surface $\rho_\infty^{-1}\langle \partial\rho/\partial z \rangle \approx \left(\sqrt{2\pi\sigma^2}\right)^{-1/2} \exp\left(-z^2/2\sigma^2\right)$ and the decay of $R(\theta)/R_F(\theta)$ with increasing θ is reminiscent of a Debye-Waller effect;

e.g., $R(\theta)/R_F(\theta) \approx \exp(-Q^2\sigma^2)$. In cases where there is some sort of layering at the surface, as for liquid crystals or certain solid surfaces, there are oscillations in the z-dependence of $\rho_\infty^{-1}\langle\partial\rho/\partial z\rangle$ and the Fourier transform of these gives rise to maxima and minima in the angular, or Q, dependence of the specular reflectivity $R(\theta)$. The real space structure of the electron density, along the surface normal, can be derived from the Q dependence of the reflectivity. In addition, diffuse scattering that can be observed by tuning the spectrometer off of the specular condition can be analyzed to measure variations in the surface structure parallel to the plane of the surface.

Some experimental studies on surface structure can be carried out on the Harvard Materials Research Laboratory Rotating Anodes X-Ray Facility, however most of the studies must eventually be completed using the higher intensity, and other properties, of synchrotron radiation. To this end a significant fraction of our experimental program is carried out on either beam line X22B, or X25 at Brookhaven National Laboratory.

In the nine months of this report period we have constructed a portable UHV load-lock and X-ray sample chamber as illustrated schematically in Figure I.1. Samples prepared in a Molecular Beam Epitaxial (MBE) growth chamber are transferred under UHV conditions to the X-ray scattering chamber that can be located at either Harvard University or at the National Synchrotron Light Source (NSLS) at Brookhaven National Laboratory.

In order to fully carry out our proposed program of characterizing buried interfaces the X-ray scattering chamber had the following design requirements. (1) It had to be capable of precise, reproducible positioning on one, or another X-ray spectrometers. (2) It had to allow for a wide range of accessible momentum transfers such that we could measure both specular reflection and surface Bragg scattering on the same sample. (3) It had to maintain satisfactory UHV pressures such that the samples were not significantly changed in the time between the MBE preparation and the measurement. The most technically challenging problem was the design and construction of

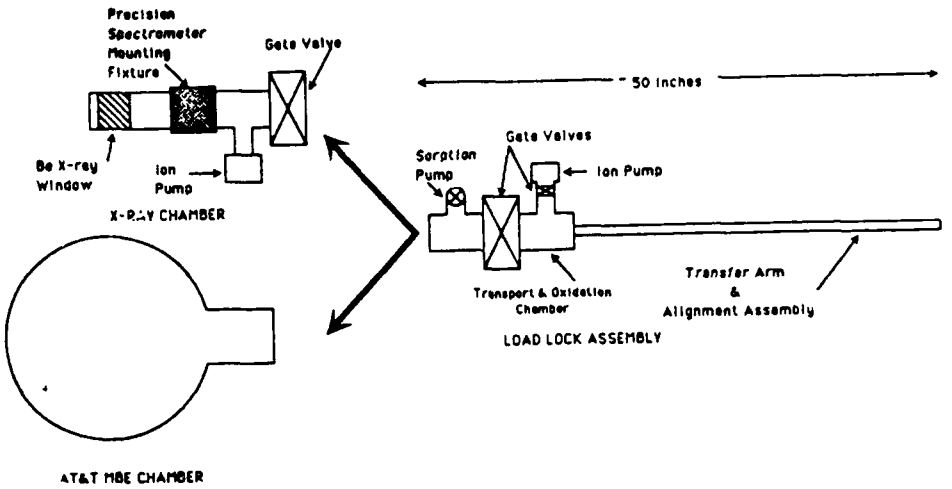

Figure 1.1. Schematic illustration of the portable load-lock assembly and the X-ray scattering chamber described in the text. The portable load-lock assembly and the X-ray scattering chamber were both designed to mate to the AT&T Molecular Beam Epitaxial Growth Chamber. In normal operation the sample is transferred to the portable load-lock assembly which will then be transported to the X-ray scattering chamber mounted on a spectrometer at either Harvard or NSLS.

the "precision mounting fixture" that would allow relatively unencumbered rotation of the chamber while maintaining reproducible sample positions to an accuracy of ~ 0.1 mm and angular positions to an accuracy of $\sim 0.005°$. In the final design the entire assembly, including valve and ion pump weighs approximately 50 pounds. The mechanical features of the mounting on the Huber 4-circle goniometer at beamline X22B at NSLS were tested in February of this year when the synchrotron was not operating.

The magnetically coupled transfer arm was particularly designed to accept samples from the MBE chamber at AT&T Bell Laboratories operated by Joze Bevk with whom we are collaborating. The ion pump power supply is a special design that can be powered by an automobile battery. In April of this year the load-lock assembly was moved to AT&T Bell Laboratories and mounted on the MBE growth chamber that is illustrated schematically in the figure. A silicon substrate with the [001] axis oriented to within 0.03° of the surface normal was prepared in an MBE growth chamber at AT&T Bell Laboratories by dry oxidation to produce an incomplete surface oxide

layer approximately 7Å thick. The sample was transferred from the AT&T growth chamber into the portable load-lock. The load-lock was maintained at a pressure of 5×10^{-9} Torr during transfer of a sample from AT&T Bell Laboratory in New Jersey to the Gordon McKay Laboratory at Harvard on May 6th of this year.

After further mechanical and vacuum tests the portable transport chamber, still containing the sample, and the X-ray scattering chamber were transported to NLSL and mounted on beamline X22B on May 11th. In the process of opening the gate valve between the portable load-lock and the X-ray scattering chamber there was a brief period when outgasing from the gate valve caused the pressure to rise to approximately 10^{-6} Torr. In view of the fact that characterization of the sample at AT&T following the X-ray measurements indicated less than 0.1 monolayer of carbon, no significant other contaminants and the approximately 7Å of SiO_2 that was expected from the growth conditions this brief exposure was of no significance.

During the allotted five days of synchrotron time NSLS experienced one major vacuum leak to the synchrotron storage ring (loss of two days of beam) and one major flood on the experimental floor (loss of one half day). In the remaining time the specular reflectivity of this sample was measured continuously over incident angles varying from grazing incidence to past the [004] Bragg peak. The results are shown in Figure I.2. The sharp peak at the forbidden [002] position is due to multiple reflection, possibly a combination of [111] and $[\bar{1}\bar{1}1]$. Although this can probably be eliminated by rotation of the sample about the [001] direction (*i.e.*, in the ϕ direction) there was not sufficient time to fully explore this effect. Similarly there was not sufficient time to probe the region of low intensity between near $Q \approx 2.6\text{Å}^{-1}$. The overall shape of this type of data, measured over 10 orders of magnitude, places severe constraints on any possible model for the surface structure.

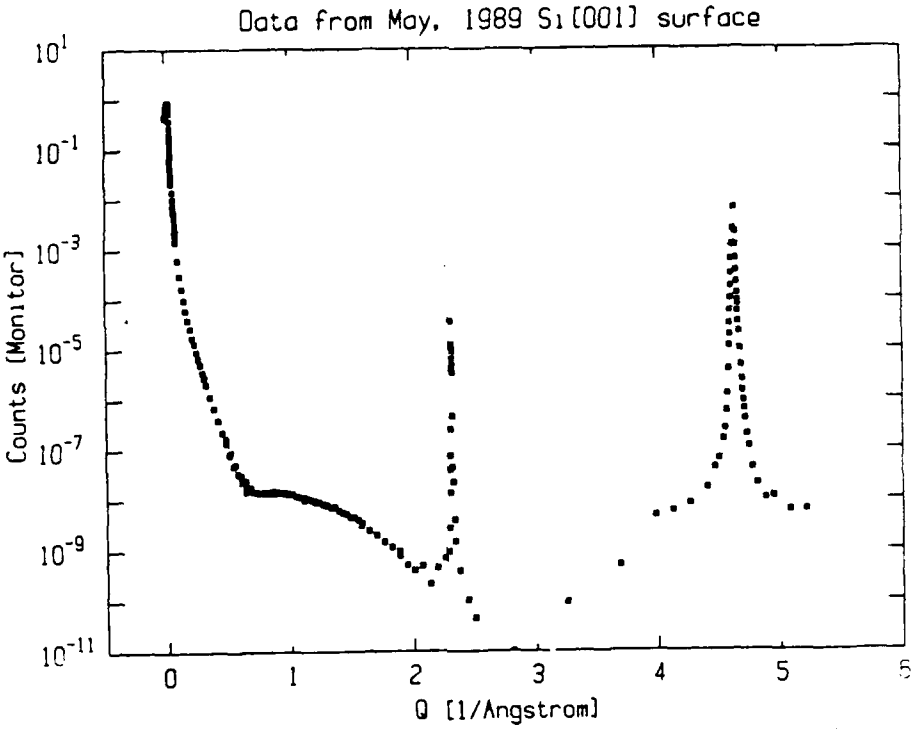

Figure I.2. X-ray specular reflectivity from the [001] face of a Si crystal coated with approximately 7 Å SiO_2. The peak near $Q \approx 4.6$ Å^{-1} corresponds to the [004] Bragg reflection. The sharper peak at $Q \approx 2.3$ Å^{-1} arises from multiple scattering such as the [111] and [$\bar{1}\bar{1}$1] and is sensitive to rotation of the sample around the [001] direction.

References:

1. See, for example, the collection of papers from the "Symposium on Interfaces and Thin Films," Proc. Nat. Acad. Sci (USA), **84**, 4665 (1987).

2. See the brief review, S. A. Rice, "X-Ray Reflection from Liquids," *Nature* **316**, 108 (1985).

3. L. G. Parratt, "Surface Studies of Solids by Total Reflection of X-Rays," *Phys. Rev.* **95**, 359 (1954).

4. R. W. James, in The Optical Principles of the Diffraction of X-Rays (ed. Sir Lawrence Bragg) (Cornell University, Ithaca, NY, 1965).

5. L. Bosio, R. Cortes, A. Defrain, and M. Qumezine, "Experimental and Theoretical Studies of the Density Profile in the Liquid-Vapor Interface of Mercury and Gallium," *J. Non-Cryst. Solids* **61/62**, 697 (1984).

6. P. S. Pershan, A. Braslau, A. H. Weiss, and J. Als-Nielsen, "Smectic Layering at the Free Surface of Liquid Crystals in the Nematic Phase: X-Ray Reflectivity," *Phys. Rev.* **A35**, 4800 (1987).

7. A. Braslau, M. Deutsch, P. S. Pershan, A. H. Weiss, J. Als-Nielsen, and J. Bohr, "Surface Roughness of Water Measured by X-Ray Reflectivity," *Phys. Rev. Lett.* **54**, 114 (1985).

8. A. Braslau, P. S. Pershan, G. Swislow, B. M. Ocko, and J. Als-Nielsen, "Capillary Waves on the Surface of Simple Liquids Measured by X-Ray Reflectivity," *Phys. Rev.* **A38**, 2457 (1988).

9. B. M. Ocko, A. Braslau, P. S. Pershan, J. Als-Nielsen, and M. Deutsch, *Phys. Rev. Lett.* **47**, 94 (1986).

10. P. S. Pershan and J. Als-Nielsen, "X-Ray Reflectivity from the Surface of a Liquid Crystal: Surface Structure and Absolute Value of Critical Fluctuations," *Phys. Rev. Lett.* **52**, 759 (1984).

11. See references 3 and 4.

ANNUAL REPORT OF

PUBLICATIONS/PATENTS/PRESENTATIONS/HONORS

a. Papers Submitted to Refereed Journals (and not yet published)

I. M. Tidswell, B. M. Ocko, P. S. Pershan, S. R. Wasserman, G. M. Whitesides, and J. D. Axe, "X-Ray Specular Reflection Studies of Silicon Coated by Organic Monolayers (alkylsiloxanes)," submitted to *Physical Review.* (Partially supported by DMR–86–14003, MRL)

S. R. Wasserman, G. M. Whitesides, I. M. Tidswell, B. M. Ocko, P. S. Pershan, and J. D. Axe, "The Structure of Self-Assembled Monolayers of Alkylsiloxanes of Silicon: A Comparison of Results from Ellipsometry and Low-Angle X-Ray Reflectivity," submitted to *Journal of American Chemical Society.* (Partially supported by DMR–86–14003, MRL)

b. Papers Published in Refereed Journals

A. Braslau, P. S. Pershan, G. Swislow, B. M. Ocko, and J. Als-Nielsen, "Capillary Waves on the Surface of Simple Liquids Measured by X-Ray Reflectivity," *Phys. Rev.* **A38**, 2457 (1988). (Partially supported by DMR–86–14003 MRL, and DMR–85–13523)

c. Books (and sections thereof) Submitted for Publication

P. S. Pershan, "Scattering from Mesomorphic Structures," (to be published in the *International Tables for Crystallography:* Vol. B).

P. S. Pershan, *Structure of Liquid Crystal Phases*, World Scientific Publishing Co., Singapore, 1988). (Partially supported by NSF Grants DMR–83–16979 and DMR–85–13523)

g. Invited Presentations at Topical or Scientific/Technical Society Conferences

I. M. Tidswell, M. V. Baker, T. A. Rabedeau, S. R. Wasserman, P. S. Pershan, and G. M. Whitesides, "Structure Determination of Alkylsiloxane Monolayer Films on Silicon by X-Ray Reflection," 21st ACS Central Regional Meeting, Cleveland, Ohio, June, 1989.

j. Graduate Students and Postdoctorals Supported Under the JSEP for the Year Ending July 31, 1989.

Dr. Tom Rabedeau, half time and Mr. Ian Tidswell.

I.4 High Temperature Superconductivity. L. Ji, G. C. Spalding, M. Iansiti, C. J. Lobb, and M. Tinkham, Grants N00014–89–J–1023, N00014–89–J–1565, and DMR–86–14003; Research Unit 4.

We have made substantial progress in our studies of harmonic generation in YBCO and in our work on point-contact tunneling into BSCCO, as described briefly below:

a) *Harmonic generation*: In this area, we have made important progress in clarifying the physical basis for the prominent harmonic generation that is observed in samples of YBCO with low critical current densities, thereby offering an alternative, and we believe definitely superior, interpretation of a wide variety of experimental phenomena. This work is summarized elsewhere in this Report as one of the Significant Accomplishments.

b) *Point-contact tunneling:* Tunneling experiments have historically been a rich source of information about superconductors, giving energy gap values, phonon frequencies, etc. The technique has proved more difficult with high-T_c materials because the short coherence length associated with high-T_c makes the tunneling particularly sensitive to surface quality on an atomic length scale. Moreover, the new materials tend to react with the atmosphere, giving rise to surfaces which do not represent intrinsic bulk material. Although some progress has been reported in making thin-film overlay junctions, the best results still seem to be achieved using a point-contact approach, which allows breaking through the surface layer, if necessary, to probe internal material.

After some initial experiments by graduate student G. C. Spalding, using an existing point-contact rig using etched Nb or NbTi points, in recent months we have shifted to using a low-temperature STM head built in a collaboration with Dr. D. W. Abraham at IBM. This unit should give us much better control of contact separation or pressure while at low temperature. In principle, we are also able to

move the point relative to the sample to probe different regions on the crystal, but the necessary computer facilities are not yet available to exercise this option conveniently. The material under study continues to be a set of small single crystals of BSCCO kindly supplied by Dr. D. E. Morris, of Lawrence Berkeley Lab. Our initial experience with this new tunneling setup has been very encouraging, but the range of I-V curves obtained is still too large to allow us to draw any firm conclusions about intrinsic properties. When these dc experiments are completed, it is planned to examine the response of contacts or constrictions at far-infrared frequencies, using our gas laser source.

I.5 Quantum and Charging Phenomena in Mesoscopic Josephson Junctions. M. Iansiti, A.T. Johnson, and M. Tinkham, Grants N00014–89–J–1023 and N0014–89–J–1565, and NSF Grant DMR–84–04489; Research Unit 4.

After publication of two Physical Review Letters and a comprehensive Physical Review article on our work on single very small junctions, as well as presentation of an Invited Paper on the work at the March Meeting of the APS, the first generation of work is drawing to a very successful completion.

One additional paper [1] has now been submitted, which extends our analysis to provide a more quantitative fit to the novel and surprising small resistance R_0 measured below the critical current I_c is these junctions. In this new work, the measured temperature dependence of R_0 is fitted to theory continuously from the classical region at higher temperatures down to the fully quantum region below 50 mK. This allows us to determine the damping parameter *experimentally* from the classical regime where it plays a significant quantitative role, and thereby show that it should have an insignificant effect in the quantum regime; this demonstrates that the junction must be largely decoupled (perhaps by impedance mismatch) from the loading effect of the characteristic impedance of the leads, as had been assumed in our earlier analysis.

In another important experimental confirmation of our earlier analysis, we have shown that the abrupt leveling off to R_0 when T is reduced to the nominal crossover temperature $T_{\rm crossover}$ can not be an artifact of extraneous noise or heating effects (rather than a crossover from classical to quantum regimes as we have claimed). We have done this by showing that this leveling off of R_0 *does not occur* in the presence of a magnetic field which reduces I_{CO} and hence should lower $T_{\rm crossover}$ below the lowest accessible temperatures. By contrast, the field should have no effect if the leveling off were due to extraneous noise or heating which prevented the actual temperature from following the nominal temperature down below the nominal $T_{\rm crossover}$. Although a comprehensive understanding of these phenomena is still lacking, these new checks continue to support the qualitative interpretation that we have presented to account for our data.

Looking ahead, we have started a series of experiments involving multiple junction configurations. These are designed to provide a better-controlled electromagnetic environment on the micron length scale, and also to permit tests of concepts for 3-terminal superconducting devices.

Reference:

1. M. Iansiti, A. T. Johnson, C. J. Lobb, and M. Tinkham, *Phys. Rev.* **B**, submitted.

I.6 High-Frequency Properties of Josephson-Junction Arrays. M. Rzchowski, S. P. Benz, C. J. Lobb, and M. Tinkham, Grants N00014–89–J–1023, N00014–89–J–1565, and DMR–84–04489; Research Unit 4.

For a number of years, we have been studying the properties of two-dimensional arrays of SNS Josephson junctions, emphasizing their use as a model system for studying the nature of the phase transition from the superconducting to the resistive state, particularly as influenced by an applied magnetic field. With our newly acquired facili-

ties for high-frequency and microwave experimentation (funded by an ONR equipment grant), we have shifted the emphasis of our work to study of the dynamic response of these systems. We are also shifting the primary support for the work from the NSF-MRL to JSEP-ONR to reflect this change in emphasis.

During the past year, we have developed the non-trivial capability of fabricating these arrays using Nb (rather than Pb) films to form the superconducting islands connected by Cu proximity effect bridges. Niobium has great advantages in robustness, so that these structures can be cycled repeatedly to helium temperatures without significant change in properties, whereas the Pb-based arrays essentially could be used only once. We have fabricated single junctions, one-dimensional series arrays of junctions, double-stranded "ladder" arrays, and fully two-dimensional square arrays. The one-dimensional arrays have typically 1000 junctions in series, while the square arrays are typically 1000 $\times$ 1000 in size, containing two million junctions. From various tests and comparisons, it is clear that our fabrication methods yield highly uniform and reproducible samples, which should allow meaningful experimental data to be obtained.

Our first round of experiments have been devoted to investigating the voltage-locking properties of such arrays of overdamped SNS junctions, when driven by rf currents at various frequencies relative to the characteristic R/L frequency of the devices. In this, R is the shunt resistance of a junction, while L is the effective Josephson inductance of its supercurrent channel. Driven below this characteristic frequency, the supercurrent channel dominates, and the device is effectively current biased. Above this frequency, the shunt dominates, and the device is effectively voltage biased.

In preliminary experiments, we have observed Shapiro steps at voltage intervals of 1000$\times$ hf/2e, indicating voltage-locking of 10^6 junctions in 2-D arrays driven at frequencies from the kHz to the MHz region, and up to the GHz range in 1-D arrays of 10^3

junctions. Under some circumstances we see subharmonic as well as integer-multiple steps, but we have not yet determined whether the subharmonic steps are due to the coupling together of multiple junctions, deviations from the ideal $\sin\varphi$ current-phase relation, on other reasons. Our experiments to date already show voltage-locking of many junctions on the same Shapiro step, but a more interesting possibility is actual *phase-locking* into a "superradiant state," which would couple strongly with the external radiation field. Tests for this behavior are planned. Inverting the role of ac and dc, if such self-synchronization and phase locking took place spontaneously under dc drive, there would be device potential as a voltage-tuneable Josephson-junction-array high frequency generator. Such devices have been demonstrated [1] in 1-D arrays, but a 2-D array would offer the possibility of much greater power output because of 1000 times more junctions; moreover, there is some evidence that self-synchronization is easier to accomplish in the 2-D geometry. Other preliminary experiments performed include study of the effect of a perpendicular magnetic field. Because of fluxoid quantization within each cell of the array, this introduces interesting critical current modulations which affect the response to the high-frequency current. Much work remains to be done.

Reference:

1. A. K. Jain, K. K. Likharev, J. E. Lukens, and J. E. Sauvegeau, *Phys. Rev.* **109**, 310 (1984).

ANNUAL REPORT OF

PUBLICATIONS/PATENTS/PRESENTATIONS/HONORS

a. Papers Submitted to Refereed Journals (and not yet published)

Q. Hu and M. Tinkham, "Power Spectra of Noise-induced Hopping between Two Overlapping Josephson Steps," *Phys. Rev.* **B**, to appear. (Partial support also from ONR Grant N00014–89–J–1565)

M. Iansiti, A. T. Johnson, C. J. Lobb, and M. Tinkham, "Quantum Tunneling and Low-Voltage Resistance in Small Superconducting Tunnel Junctions," *Phys. Rev.* **B**, submitted. (Partial support also from ONR Grant N00014–89–J–1565, and from NSF Grant DMR–84–04489)

L. Ji, R. H. Sohn, G. C. Spalding, C. J. Lobb, and M. Tinkham, "Critical State Model for Harmonic Generation in High Temperature Superconductors," *Phys. Rev.* **B**, submitted. (Partial support also from ONR Grant N00014–89–J–1565, and from NSF Grants DMR–84–04489 and DMR–86–14003)

b. Papers Published in Refereed Journals

M. Tinkham, "The Resistive Transition of High Temperature Superconductors," *Phys. Rev. Lett.* **61**, 1658–1661 (1988). (Partial support also from ONR Grant N00014–89–J–1565, and from NSF Grants DMR–84–04489 and DRM–86–14003)

M. Iansiti, M. Tinkham, A. T. Johnson, W. F. Smith, and C. J. Lobb, "Charging Effects and Quantum Properties of Small Superconducting Tunnel Junctions," *Phys. Rev.* **B39**, 6465–6481 (1989). (Partial support also from ONR Grant N00014–89–J–1565, and from NSF Grant DMR–84–04489)

M. Iansiti, A. T. Johnson, C. J. Lobb, and M. Tinkham, "Response to Comment on 'Crossover from Josephson Tunneling to the Coulomb Blockade in Small Tunnel Junctions'," *Phys. Rev. Lett.* **62**, 484 (1989).

d. Books (and sections thereof) Published

M. Tinkham and C.J. Lobb, "Physical Properties of the New Superconductors," Chapter in *Solid State Physics*, Vol. 42, published by Academic Press, pp. 91–134 (1989). (Partial support also from ONR Grant N00014–89–J–1565 and from NSF Grant DMR–84–04489)

g. Invited Presentations at Topical or Scientific/Technical Society Conferences

M. Tinkham, "Considerations Limiting Critical Currents in High Temperature Superconductors," ISTEC Workshop on Critical Currents in High T_c Superconductors, Oiso, Japan, February, 1989.

M. Tinkham, "Charging Effects, Quantum Tunneling, and Dissipation in Small Superconducting Tunnel Junctions," March Meeting of APS, St. Louis, March 1989.

i. Honors/Awards/Prizes

M. Tinkham was chosen as Academic Exchange Visitor by Academia Sinica, giving lectures in Institute of Physics in Beijing, University of Science and Technology of China in Hefei, and at Fudan University in Shanghai, October 1988.

Chosen as "Hilldale Lecturer" at University of Wisconsin, Madison, April 1989.

Chosen as Chairman of Gordon Research Conference on *Phenomenology of High Temperature Superconductors*, Wolfeboro, NH, June, 1989.

Chosen as member of Scientific Advisory Board of American Superconductor Corp., and of Hypres Corporation.

j. Graduate Students and Postdoctorals Supported Under the JSEP for the Year Ending July 31, 1989.

Dr. M. Rzchowski and Mr. S. P. Benz. (Note: Five other students share JSEP facilities, but have no JSEP salary.)

I.7 Nonlinear Dynamics of Electronic Neural Networks.

K. L. Babcock, C. Marcus, and R. M. Westervelt, Grant N00014–84–K–0465; Research Unit 5.

The mathematical tools developed to analyze nonlinear dynamical systems can also be used to understand the dynamics of electronic neural networks for which nonlinearity is essential. Neural networks comprised of analog neurons with a smooth transfer function — or so called response — are widely used as models of real biological neural systems as well as in analog VLSI implementations of neural networks (see for example, Mead [1]). However, much of the theoretical basis of neural network design is derived from a more schematic model where a neuron is taken to be a binary (0,1) threshold element [2]. Because binary neurons can be treated as Ising spins, the formalism of spin-glass theory has been used with considerable success to analyze the static properties of binary neural networks [3]. Unfortunately, the dynamics and stability of neural networks are not well treated by spin-glass theory and remain relatively unexplored. Furthermore, the applicability of the many recent spin-glass results to electronic neural networks has not been explored in any detail. These issues become especially important as analog VLSI fabrication is used more widely.

In the past year, we have continued our study of electronic neural networks as nonlinear dynamical systems, paying particular attention to the role of the neuron's nonlinear transfer function in the design of fast, stable analog networks. We find in many cases that analog networks are more versatile and well-behaved than their binary counterparts. In Marcus and Westervelt [4], we prove two important properties of analog neural networks updated in parallel as iterated maps. First, for symmetric interconnections and for a very broad class of neuron transfer functions, these networks possess only two types of attractors: fixed points and period–two limit cycles. Second, by lowering the gain (maximum slope) of the neuron transfer function below a critical value, all period-two attractors can be eliminated. This result can be stated as a global stability criterion relating the maximum allowed gain to the most negative eigenvalue

of the connection matrix.

This result demonstrates the value of analog computation for such tasks as associative memory. Associative memory networks made from binary neurons are plagued with oscillation when updating is done in parallel, forcing one to use slow — but stable — serial updating. In contrast, analog neural networks satisfying the above stability criterion can be rapidly updated in parallel with guaranteed convergence to a fixed point. These results have been further generalized to allow a more liberal stability criterion at the expense of an updating scheme based on multiple previous states of the network [5].

We have also shown that lowering the neuron gain has the additional benefit of reducing the number of spurious attractors [6], similar to annealing effects seen in Monte Carlo dynamics. Unlike Monte Carlo methods, this form of "analog annealing" is completely deterministic, depending only on the neuron transfer function, and can be easily implemented using analog electronics.

We have completed a systematic study of the effects of time delay in analog neural networks [7] which investigates the influence of network topology on stability and shows that certain topologies are quite sensitive to small neuron "gate delays." For too great a delay, networks with feedback tend to develop a type of "epilepsy" in which all neurons oscillate together. We have also shown experimentally that chaotic attractors can be created by adding time delay to the response of a single analog neuron in a small, otherwise nonchaotic electronic network. These results [8] contrast with recent results for discrete-time binary networks for which long-period attractors are quite rare (Gutfreund *et al.*, 1988). By highlighting the important role of delay in producing chaotic dynamics, these results may also be useful in constructing realistic models of chaotic dynamics observed in real neural systems (see, for example, Skarda and Freeman [10]).

References:

1. C. A. Mead, *VLSI and Neural Systems* (Addison, Wesley, Reading, MA, 1989).
2. J. J. Hopfield, Proc. Nat. Acad. Sci. USA **79**, 2554.
3. D. J. Amid, H. Gutfreund, and H. Sompolinsky, *Ann. Phys.* **173**, 30 (1987).
4. H. Gutfreund, J. D. Reger, and A. P. Young, *J. Phys.* **A21**, 2775 (1988).
5. C. M. Marcus and R. M. Westervelt, *Phys. Rev.* **A40**, 501 (1989c).
6. C. M. Marcus and R. M. Westervelt, to be published (1989d).
7. C. M. Marcus, F. R. Waugh and R. M. Westervelt, to be published, (1989b).
8. C. M. Marcus and R. M. Westervelt, *Phys. Rev.* **A39**, 347 (1989a).
9. C. M. Marcus and R. M. Westervelt, in *Advances in Neural Information Processing Systems*, Denver CO (ed. D. Touretzky) (Morgan Kauffman, San Mateo, CA, 1989b), p. 568.
10. C. A. Skarda and W. F. Freeman, *Behav. and Brain Sci.* **10**, 161 (1988).

ANNUAL REPORT OF

PUBLICATIONS/PATENTS/PRESENTATIONS/HONORS

a. Papers Submitted to Refereed Journals (and not yet published)

S. H. Strogatz, C. M. Marcus, R. M. Westervelt, and R. E. Mirollo, "Collective Dynamics of Coupled Oscillators with Random Pinning," *Physica* **D**, submitted.

C. M. Marcus and R. M. Westervelt, "Dynamics of Iterated Map Neural Networks," *Phys. Rev.* **A**, in press.

C. M. Marcus and R. M. Westervelt, "Dynamics of Analog Neural Networks with Time Delay," in *Advances in Neural Information Processing Systems* (Morgan Kaufman, San Mateo, California, 1989), in press.

C. M. Marcus, S. H. Strogatz, and R. M. Westervelt, "Delayed Switching in a Phase-slip Model of Charge-Density Wave Transport," *Phys. Rev.* **B**, submitted.

K. L. Babcock and R. M. Westervelt, "Elements of Cellular Domain Patterns in Magnetic Garnet Films, *Phys. Rev.* **B**, in press.

K. L. Babcock and R. M. Westervelt, "Topological Melting of Cellular Domain Lattices in Magnetic Garnet Films," *Phys. Rev. Lett.*, submitted.

S. H. Strogatz and R. M. Westervelt, "Predicted Power Laws for Delayed Switching of Charge-Density Waves," *Phys. Rev.* **B**, submitted.

b. Papers Published in Refereed Journals

S. H. Strogatz, C. M. Marcus, R. M. Westervelt, and R. E. Mirollo, "Simple Model of Charge-Density Wave Dynamics with Phase Slippage," *Phys. Rev. Lett.* **61**, 2380 (1988).

C. M. Marcus and R. M. Westervelt, "Stability of Analog Neural Networks with Delay," *Phys. Rev.* **A39**, 347 (1989).

g. Invited Presentations at Topical or Scientific/Technical Society Conferences

R. M. Westervelt and C. M. Marcus, "Stability of Neural Networks with Delay," *Neural Networks for Computing*, Snowbird, Utah, 4/4/89 to 4/8/89.

R. M. Westervelt and K. L. Babcock, "Pattern Formation of Magnetic Domains," Spring School on Experimental Nonlinear Dynamics, Tianjin, China, 5/8/89 to 5/12/89.

C. M. Marcus, "Dynamics of Iterated Map Neural Networks," A.I.P. Topical Conference on Computational Physics, Boston, 6/18/89.

h. Contributed Presentations at Topical or Scientific/Technical Society Conferences

C.M. Marcus and R.M. Westervelt, "Dynamics of Analog Neural Networks with Time Delay," Neural Information Processing Systems, Denver, 11/89.

K. L. Babcock and R. M. Westervelt, "Elements of Cellular Domain Patterns in Magnetic Garnet Films," March Meeting of the American Physical Society, St. Louis, 3/20/89 to 3/24/89.

j. Graduate Students and Postdoctorals Supported Under the JSEP for the Year Ending July 31, 1989.

K. L. Babcock, C. M. Marcus (Bell Scholar, no salary support), and F. Waugh.

I.8 Structural and Electronic Studies of Semiconductor Interfaces and Surfaces J. A. Golovchenko, Grant N00014–89–J–1023, Conracts N00014–87–K–0511, and NSF–DMR86–14003; Research Unit 6.

In the JSEP proposal covering this three year period, the stated objective of unit 6 was to study and correlate structural and electronic properties of semiconductor interfaces and provide new insight into homo- and heteroepitaxial crystal growth, interface junctions and electrical processes into and along interfaces, with an emphasis of understanding the physics and chemistry of related phenomena on length scales below 100 Å.

Effective use of JSEP funds for this purpose was to hinge upon use of three major facilities at Harvard; the tunneling microscope, tandem ion accelerator and X-ray interferometry facility. At the time of the proposal only the tunneling microscope project was capable of contributing to the stated objective. The accelerator had no UHV beamlines or scattering chamber and DOE funding of the X-ray facility was on hold.

Since that time the tunneling microscope has continued to make progress towards our objective. The UHV beamline on the tandem accelerator has been completed and outfitted with a UHV scattering chamber. The chamber has itself been outfitted with a variety of UHV surface preparation and analysis capabilities (*i.e.*, effusion ovens, sputter cleaning, LEED and sample heating and cooling). Finally, the X-ray facility funding by the DOE has been approved and will begin August 15. Since this research involves collaboration with Bell Laboratories, they have already supplied a UHV chamber for this effort and opportunities for research to be performed on the Bell Laboratories beamline at the Synchrotron Light Source at Brookhaven National Laboratory.

Given the above constraints our initial studies have focused on two problems, the study of boron atoms on Si(111) surfaces and Ge epitaxy on silicon surfaces.

Boron is an acceptor impurity in bulk silicon and only recently has it become clear that it plays an interesting role in the reconstruction of clean silicon surfaces. Our surface studies suggest that it may be a good case for MBE bulk doping during crystal growth as well as atomic scale programming for achieving controlled doping profiles over very small distances near the surface.

Initial studies were performed with the tunneling microscope on (111) silicon surfaces. Samples doped to $\sim 10^{20}$ B/cm^3 were thermally annealed to temperatures of 1,000–1,100 °C after which boron atoms had segregated at the surface as measured by Auger spectroscopy. LEED showed a strong $\sqrt{3} \times \sqrt{3}$ R30° reconstruction of the surface, in agreement with the work of Reference [1]. Our tunneling microscope studies concentrated first on identifying the surface atomic species and the electronic structure of various points on the surface. Atomic scale topographs showed two types of ad-atom structure on $\sqrt{3} \times \sqrt{3}$ T4 sites.

Both for the purposes of identifying the two types of structures and for later RBS boron surface coverage studies, it was decided to develop a sputtering atomic source for boron deposition on undoped samples and a silicon evaporation source for regrowth studies above boron deposited layers. Both sources were operated in the tunneling microscope chamber.

These atomic sources allowed the experimental identification of boron and silicon type sites on $\sqrt{3} \times \sqrt{3}$ mixed surfaces. It turns out (using our experiments and calculation of David Vanderbilt) that silicon atoms occupy ad-atom sites above the last (111) atomic double layer, where group III elements would normally be expected, and, somewhat surprisingly, boron atoms lie in the lower plane of the last double layer directly under the surface silicon ad-atoms. Silicon ad-atoms seem also to be able to occupy $\sqrt{3} \times \sqrt{3}$ ad-atom positions with boron atoms below on the mixed surface.

These two types of states have been characterized electrically by tunneling dI/dV measurements. The boron atom sites have a major unoccupied localized surface state $\sim$ 1.5 eV above the Fermi Level. The silicon sites have a very similar electronic structure to those on 7×7 reconstructions, which have a particularly low density of states at that energy.

Equally interesting from a practical point of view is the fact that our boron layers are easily covered by subsequent silicon epitaxy which leads to virgin 7×7 reconstructions after just a few monolayers. Figure I.3 shows the first tunneling microscope images of this epitaxy process. This shows that boron atoms can be effectively incorporated as dopants during the epitaxy process. This is in distinction to both gallium and arsenic atoms, which either evaporate or continuously segregate at the surface during epitaxy.

Accurate boron surface coverages have been notoriously difficult for us to establish by the retarding field Auger spectrometer in our tunneling chamber. Therefore a parallel project on the Tandem Accelerator has begun to take advantage of a boron $(p-\alpha)$ nuclear reaction. Ion implanted calibration samples from Bell Laboratories have been obtained and a solid state detector system implemented on the general purpose beamline that is capable of determining boron monolayer coverages with better than 10% accuracy. This capability will shortly be integrated with the tunneling studies.

Preliminary crystal epitaxy studies have also begun on the UHV tandem accelerator beamline. First the system had to be brought to the condition where standard 7×7 and 2×1 reconstructions could be routinely obtained on silicon substrate surfaces, together with clean RBS and channeling spectra. Subsequently enough experience with our new effusion cell design was obtained so that monolayer coverages of gallium and arsenic could be deposited with the expected surface LEED pattern being obtained. Finally an *e*-beam evaporator was made operational for germanium depositions on clean and surface-doped substrates.

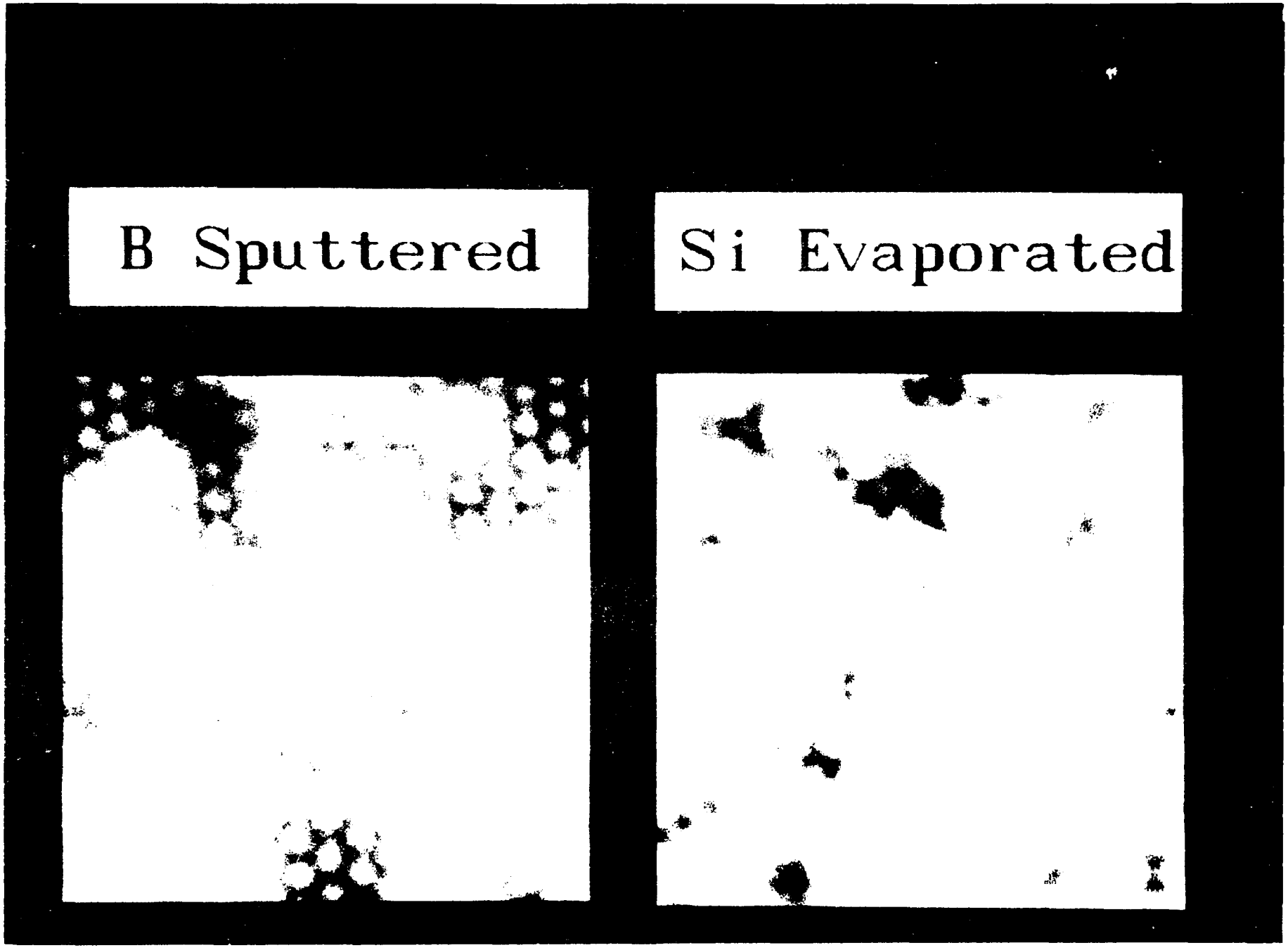

Figure 1.3. Tunneling images of boron doped surfaces of silicon. All observed surface atoms are silicon. Dark atoms have boron sites directly below. Bright ones have silicon below. First image after boron monolayer doping. Second image after subsequent silicon monolayer epitaxial growth.

Our early experiments have been geared towards studying the effect of surface doping on the molecular beam epitaxy process. Consequently germanium epilayers have been grown on a variety of surfaces doped with boron, gallium and arsenic atoms. Our immediate goal has been to see if such doping can stop the islanding of germanium known to occur on this surface after a few initial pseudomorphic atomic planes are laid down.

We initially planned to use only the signal from the shadowed silicon channeling surface peak as our indicator of the area between germanium islands on the surface. Good planar growth was anticipated to yield complete silicon surface peak suppression after several tens of atomic layers were grown. This condition was never realized under a wide variety of growth conditions studied. To elucidate our problems, images of the surface were obtained with a scanning electron microscope. The islanding expected was quite generally observed. In a few cases with arsenic doping, however, relatively smooth planar growth was observed in the microscope. The conditions for this growth, in which arsenic follows the surface, and the reasons for the lack of silicon peak suppression in the channeling studies are under investigation.

We hope to make progress in this area with Monte Carlo computer studies of the channeled particle motion through the SiGe interface as a function of Ge overlayer thickness. A student on this project, Nancy Hecker, is spending the summer at Bell Laboratories, developing the software under the collaborative guidance of L. C. Feldman. We are also progressing towards directly imaging the surface as a function of growth on the tunneling microscope. A second student, Mike Pravika, will be spending the summer with J. R. Patel of Bell Laboratories at the Synchrotron Radiation Source at BNL studying the problem with X-ray standing waves.

Finally the UHV chamber provided by Bell Labs for the X-ray collaboration at Harvard has been made operational from the standpoint of attaining 10^{-10} Torr vacuum levels. While this facility awaits integration in the soon-to-be funded DOE

project, Robert Martinez has been using it to develop a method to evaluate surface stresses associated with monolayer surface physics and epitaxial growth problems. Such stresses play a major role in determining surface reconstructions and conditions under which strained epilayers may grow. For this study extremely thin waters ($\sim 2 - 4 \times 10^{-3}$ in.) are prepared with clean surfaces in the chamber and are dosed on opposite sides differently. The imbalanced surface stress leads to a bending of the surface which can be sensitively detected by optical means. Samples have been prepared, a manipulator and oven fabricated, and the optical system is operational. On paper the experimental sensitivity is 10–100 times that needed to detect the surface stress difference between arsenic terminated and Si 7×7 surfaces. We shall soon see.

Finally we are continuing to recruit graduate students to participate in the new JSEP research. We also have just filled a postdoctoral position with an experienced ion-implantation and accelerator person from Cal. Tech., who will work full time on the epitaxial crystal growth project earlier discussed.

Reference:

1. V. V. Korobsov, V. G. Lifshits, and A. B. Zotov, *Surf. Sci.* **195**, 466 (1988).

ANNUAL REPORT OF
PUBLICATIONS/PATENTS/PRESENTATIONS/HONORS

j. Graduate Students and Postdoctorals Supported Under the JSEP for the Year Ending July 31, 1989.

Mr. R. Martinez

II. QUANTUM ELECTRONICS

Personnel

Prof. N. Bloembergen
Assoc. Prof. E. Mazur
Dr. M. Buijs
Mr. K. H. Chen
Mr. P. Saeta
Mr. J. K. Wang
Mr. J. P. Wang

II.1 Interaction of Ultrashort Laser Pulses with Semiconductor Surfaces. N. Bloembergen, E. Mazur, M. Buijs, P. Saeta, and J. K. Wang, Grant N00014-89-J-1023 and Contract NSF DMR-8858075; Research Unit 7.

Ultrashort laser pulses offer unique opportunities for studying the electronic and material properties of semiconductors and metals. Because of the small penetration depth of the laser light in such materials, and because thermal diffusion is negligible for times shorter than ten picoseconds, subpicosecond laser irradiation concentrates the laser pulse energy in a very thin layer at the surface of the material. At high pulse energies the melting threshold can thus easily be reached, and the material at the surface can transform into short-lived phases that can sometimes not be obtained by any other method. At pulse energies below the melting threshold, measurements on a femtosecond timescale probe the carrier and lattice dynamics of the material — a topic of high current interest because of the technological applications of high-speed electronics.

Until this reporting period we have been using picosecond Nd:YAG laser pulses to study the dynamics of nonequilibrium carrier relaxation as well as phase transformations in semiconductors. In recent years the advent of the colliding-pulse-mode-locked (CPM) dye laser, which produces a 100-MHz stream of roughly 100-fs, pulses has pushed the time-resolution of this type of studies by three orders of mag-

nitude. Femtosecond optical techniques have been used extensively, for instance, to study the dynamics of nonequilibrium carrier relaxation in GaAs. During this reporting period we worked on two fronts: 1) We continued the ongoing studies on a picosecond scale and 2) we built a new high-energy femtosecond laser facility.

During the first half of this reporting period we performed single-shot reflectivity measurements of the laser melting of silicon [1,2]. While numerous investigations on the phase transition of silicon during ultrafast laser annealing have been performed in recent years, the standard picosecond pump-and-probe measurements have a number of inherent drawbacks. First, they cannot resolve reflectivity changes that occur on a time scale of a few picoseconds, because they integrate over the duration of the probe pulse (typically 20 ps or more). Second, they determine the time profile of the reflectivity at fixed pump fluence in a stepwise manner by varying the delay between the pump and the probe pulse. This introduces a large amount of scatter in the data points because of shot-to-shot variations in the pump fluence, and requires a large amount of data to be taken for every time profile of the reflectivity. Third, they provide no spatial information on the melting process.

To obtain both spatial resolution and better time resolution, and to measure the time profile of the reflectivity on a single-shot basis, we measured the reflectivity of silicon during melting in a single laser-shot using a streak camera with a time resolution of 1.8 ps. To enhance the sensitivity of our measurements, the probe pulse was *p*-polarized and the probe angle of incidence was 65°, close to Brewster's angle. At this angle the reflectivity of solid silicon is small (about 10%), leading to an increase in reflectivity on melting by a factor of 8.

The high time resolution of the streak camera enabled us to confirm that the reflectivity follows the trend predicted by numerical simulations of heating above the melting temperature in silicon [3]. According to a Drude model one expects a decrease in reflectivity of molten silicon when it is heated above the melting

temperature. A numerical solution of the one-dimensional heat equation shows that at this fluence the temperature of the liquid silicon exceeds the melting temperature by more than 1000 K.

During the second part of this reporting period we built an Argon-ion laser pumped CPM dye-laser. Autocorrelation traces of the laser pulses show that the laser pulse width is about 70 fs — an improvement of almost three orders of magnitude over the previously available Nd:YAG laser pulses.

Because of the low average output power of the laser, we were initially restricted to studying electron and phonon dynamics in materials at very low excitation energy. We therefore attempted to perform femtosecond time-resolved Raman spectroscopy on Si, and other homopolar semiconductors, to probe in real-time the phonon cascade which dominates the energy-relaxation process. A similar technique has been used on a picosecond timescale to monitor the time-dependence of the LO-phonon population in GaAs [4]. While we were able to obtain Raman spectra on a femtosecond time-scale, the spectra showed no dependence on the time-delay between pump and probe pulse, because the available power was too low to induce any significant changes in the phonon population.

At present we were building a multi-stage Nd:YAG pumped amplification chain for the new femtosecond laser. Four of the stages will be used to amplify the laser pulses from the CPM laser. These four stages will be followed by a Kerr cell for continuum generation of radiation. By focusing the amplified femtosecond pulses into this cell, broadband "white" light is generated because of self-phase modulation and other nonlinear optical effects. These continuum pulses, which will be amplified in two more amplifier stages, are ideally suited for probing the reflectivity of materials undergoing phase changes because of their wide wavelength range. The new setup will thus generate femtosecond laser pulses of high energy (up to 1 mJ) over a broad range of wavelengths. The construction of the amplifier is

expected to be complete in July 1989. Together with the Raman detection technique described above the new femtosecond facility will open the door to a whole new array of experiments.

Because of the higher energy it will be possible to extend the laser melting experiments done previously under JSEP sponsorship to the femtosecond domain — a still relatively unexplored area. An interesting candidate for study is the recently reported "molten" phase of graphite after irradiation with ultrashort laser pulses [5]. While most semiconductors undergo a transition to a metallic state under laser melting, there has been disagreement as to whether the molten phase of graphite is metallic. An ellipsometric measurement at a single wavelength performed by us a few years ago, indicated a nonmetallic liquid phase. For an unambiguous determination of the electrical properties of molten graphite, it is necessary to perform the ellipsometry over a broad range of wavelengths. This will determine the contributions of free and bound electrons to the dielectric function.

High intensity femtosecond pulses can also exploit the nonlinear optical properties of materials. For example, surface second harmonic generation can be used to probe the disordering of the surface during laser irradiation with femtosecond time resolution [6]. In the case of graphite, this would provide additional information on structural changes during phase transformation.

Finally, both the melting process and carrier dynamics can be studied using the time-resolved Raman scattering technique mentioned above. Since different carbon structures show different Raman shifts, one expects that the Raman spectrum of graphite will reflect any structural transformations during melting.

References:

1. J. K. Wang, P. Saeta, M. Buijs, A. M. Malvezzi and E. Mazur, in *Ultrafast Phenomena VI* (Springer, 1989), p. 236.

2. J. K. Wang, P. Saeta, M. Buijs, and E. Mazur, *Proc. ECS Meeting*, in press.

3. P. M. Fauchet and K. D. Li, *Mat. Res. Soc. Symp. Proc.* **100**, 477 (1988).

4. J. C. Tsang, J. A. Kash, and S. S. Jha, *Physica* **B134**, 184 (1985).

5. A. M. Malvezzi, N. Bloembergen, and C. Y. Huang, *Phys. Rev. Lett.* **57**, 146 (1986).

6. H. Tom, G. Aumiller, and C. Brito-Cruz, *Phys. Rev. Lett.* **60**, 1438 (1988).

ANNUAL REPORT OF

PUBLICATIONS/PATENTS/PRESENTATIONS/HONORS

a. Papers Submitted to Refereed Journals (and not yet published)

J. K. Wang, P. Saeta, M. Buijs, and E. Mazur, "Laser Melting of Silicon: The First Few Picoseconds," *J. Electr. Chem. Society*, in press.

d. Books (and sections thereof) Published

N. Bloembergen, "Time Reversal and Spatial Inversion in Magneto-Electric and Other Nonlinear Optical Phenomena," International Symposium of Space-time Symmetries, (eds. Y. S. Kim and W. W. Zachary) (Elsevier, Amsterdam, 1989) pp. 283–289, (reprinted from *Nuclear Physics* **B**, *Proc. Suppl.* (6), 1989).

J. K. Wang, P. Saeta, M. Buijs, M. Malvezzi, and E. Mazur, "Single Shot Reflectivity Study of the Picosecond Melting of Silicon Using a Streak Camera," in *Ultrafast Phenomena VI* (Springer, 1989), p. 236.

g. Invited Presentations at Topical or Scientific/Technical Society Conferences

N. Bloembergen, "The Historical Relationship between Nonlinear Optics and Condensed Matter," American Physical Society Meeting, St. Louis, MO, March 1989.

N. Bloembergen, "Commercial Laser Applications," Banquet speech, Ninth International Conference of Laser Spectroscopy, Bretton Woods, NH, June 1989.

h. Contributed Presentations at Topical or Scientific/Technical Society Conferences

J. K. Wang, P. Saeta, M. Buijs, M. Malvezzi and E. Mazur, "Single Shot Reflectivity Study of the Picosecond Melting of Silicon Using a Streak Camera," International Conference on Ultrafast Phenomena VI, Kyoto, Japan, July 1988.

J. K. Wang, P. Saeta, M. Buijs, and E. Mazur, "Laser Melting of Silicon: the First Few Picoseconds," Nonlinear Optics Symposium of the Electrochemical Society Meeting, Chicago, October 1988.

i. Honors/Awards/Prizes

N. Bloembergen was elected Vice-President of the American Physical Society. He will serve as President-elect in 1990 and as President in 1991.

II.2 Multiphoton Vibrational Excitation of Molecules. E. Mazur. J. Wang, and K. H. Chen, Grant N00014-89-J-1023 and Contract ARO DAAL03-88-K-0114; Research Unit 8.

In this research unit the dynamics of infrared multiphoton excited polyatomic molecules is studied by time-resolved multiplex coherent Raman scattering. During the past reporting period we performed a series of measurements with the new coherent anti-Stokes Raman spectroscopy (CARS) setup, and a new supersonic molecular beam machine was put into operation. One of the graduate students involved in this project, J. Wang, obtained the Ph.D. degree with a thesis on spontaneous Raman scattering measurements of infrared multiphoton excited molecules. Dr. Wang is currently holding a postdoctoral appointment at the Massachusetts Institute of Technology.

The CARS setup was improved in several ways: 1) the spectral resolution has been increased by a factor 10 by narrowing the linewidth of the Nd:YAG laser, 2) in addition to the vibrational CARS spectrum it is now possible to obtain the pure rotational CARS spectrum by a simple change in the beam configuration, and 3) the detection system was redesigned and a Hamamatsu streak camera was incorporated into the setup to increase sensitivity and to make it possible to carry out single-shot measurements. We can now measure CARS spectra at pressures as low as 1 Torr in the bulk (or a corresponding low density in the supersonic beam), with a time-resolution of about 4 ns and a spectral resolution of approximately 0.2 cm^{-1}.

The most significant improvement to this research project, however, is the addition of the supersonic molecular beam apparatus. The adiabatic cooling of the molecules in the beam expansion has two effects: 1) The collisional rate of the molecules is greatly reduced because of the translational cooling, and 2) far fewer rotational and vibrational states are populated, greatly simplifying the analysis of

the data.

Pure rotational CARS spectra of N_2 in the beam show that at a distance of 20 mm from the nozzle the rotational temperature is reduced to below 5 K. At this temperature only the $J = 0$ and $J = 1$ states are significantly populated. Similar low temperatures have been observed for other molecules.

During this reporting period we completed our measurements on infrared multiphoton excited OCS in the bulk [1] and extended these measurements to supersonic beams. In addition we performed preliminary pure rotational CARS measurements on C_2H_4 and SF_6. The OCS molecule has three vibrational degrees of freedom. The overtone of the ν_2 mode at 527 cm^{-1} can be pumped by the CO_2 laser. Because of the cross-anharmonicity of the two modes, the population in the ν_2 mode can be monitored by observing the coherent anti-Stokes signal from the ν_1 mode at 859 cm^{-1}.

In the bulk it was found that after excitation with 100 ns CO_2 laser pulses the distribution within the ν_2 ladder is nearly equilibrium at all but the highest excitation. In fact, even though the laser only populates the first overtone level ($\nu = 2$), the distribution equilibrates *extremely* rapidly because of collisions. This rapid equilibration occurs mostly within the ν_2 ladder — very little transfer of energy to other modes (*e.g.*, the ν_1 mode) is observed. Thus, OCS provides a convenient way to study the interaction of a nearly isolated anharmonic oscillator with monochromatic infrared photons. In the bulk the excitation is mostly collisional. From the time-dependence of the peak intensities in the CARS spectrum we were able to determine the collisional relaxation of the energy in the ν_2 mode.

The measurements in the molecular beam show that most of the infrared multiphoton excitation of OCS is indeed collisional. The ground state depletion steadily decreases as the distance from the probing region to the nozzle is increased.

This happens because as the distance is increased, the gas becomes cooler and more dilute and the collision rate decreases. At a distance of about 40 mm, the depletion become constant and independent of the distance, showing that there is a small collisionless contribution to the infrared multiphoton excitation. In this collisionless regime the CARS spectrum shows a peak only at the pumped $\nu_2 = 2$ overtone. The transfer to other states in the vibrational ladder only occurs during collisions.

We are currently studying the pure rotational CARS spectrum of OCS in the beam. When these measurements are completed we plan to measure other molecular systems and to continue to improve the current apparatus. For instance, shorter infrared pulses will be used to excite the molecules, and subnanosecond time-resolution will be obtained on a single-shot basis by using the time-dispersion of the streak camera.

Reference:

1. K. H. Chen, C. Z. Lü, L. A. Avilés, E. Mazur, N. Bloembergen, and M. A. Shultz, *J. Chem. Phys.*, in press.

ANNUAL REPORT OF

PUBLICATIONS/PATENTS/PRESENTATIONS/HONORS

a. Papers Submitted to Refereed Journals (and not yet published)

K.-H. Chen, C.-Z. Lũ, L. A. Avilés, E. Mazur, N. Bloembergen, and M. A. Shultz, "Multiplex CARS Studies of Infrared Multiphoton Excited OCS," *J. Chem. Phys.*, accepted for publication.

b. Papers Published in Refereed Journals

E. Mazur, "Can Chemical Reactions be Controlled with Picosecond Infrared Pulses?" *J. Elect. Chem. Soc.* **35**, C386 (1988). (Partially supported by N00014–89–J–1023 and ARO DAAG29–85–K–0060)

d. Books (and sections thereof) Published

J. Wang, K. H. Chen, E. Mazur, "Energy Localization in Infrared Multiphoton Excited CF_2Cl_2 Studied by Time Resolved Raman Spectroscopy," Int. Conf. Quantum Electronics 1988, Tokyo Japan, Tech. Digest, p. 496. (Partially supported by N00014–89–J–1023 and ARO DAAG29–85–K–0060

g. Invited Presentations at Topical or Scientific/Technical Society Conferences

E. Mazur, "Can Chemical Reactions be Controlled with Picosecond Infrared Lasers?" Annual Meeting of the Electrochemical Society, Chicago, 1988.

h. Contributed Presentations at Topical or Scientific/Technical Society Conferences

J. Wang, K. H. Chen and E. Mazur, "Energy Localization in Infrared Multiphoton Excited CF_2Cl_2 Studied by Time Resolved Raman Spectroscopy," Int. Conf. Quantum Electronics 1988, Tokyo, Japan, June 1988. (Partially supported by N00014–89–J–1023 and ARO DAAG29–85–K–0060

j. Graduate Students and Postdoctorals Supported Under the JSEP for the Year Ending July 31, 1989.

Graduate Students: K.-H. Chen, full-time; Ph.D. end summer 1989.

III. INFORMATION ELECTRONICS: CIRCUITS AND SYSTEMS

Personnel

Asst. Prof. J. J. Clark
Prof. Y. C. Ho
Assoc. Prof. D. D. Yao
Dr. S. Strickland
Dr. P. Q. Tang
Dr. J. Zhang
Mr. G. Feigen
Mr. M. Fu
Mr. D. Friedman
Mr. J. Q. Hu
Mr. T. L. Hwang
Mr. L. Y. Shi
Mr. A. Strassberg
Mr. J. Velyvis
Mr. B. Zhang

III.1 CMOS Current Mode Implementation of Neural Network Structures.

J. J. Clark, Grant N00014-89-J-1023 and Contract NSF-CDR-85-00108; Research Unit 9.

Our work in the first nine months of the current Harvard JSEP program has proceeded on a number of fronts towards our goal of investigating the design and construction of CMOS neural network structures and their application to sensor processing tasks. The progress made in each of these avenues of research is described in the following sections.

Current Mode Realizations of Adaptive Electronic Neural Networks, Discrete Synaptic Weights — We have developed a CMOS current mode circuit that implements a standard neural element (i.e., weighted summation of inputs followed by a nonlinear sigmoidal amplifier) having discrete weights. The "synapses" are constructed from a set of binary weighted current mirrors which perform multiplication of currents by coefficients presented as a digital word (5 bits in our implementation). The building blocks that make up this neural element have been fabricated through the MOSIS facility and are currently being characterized.

Current Mode Realizations of Adaptive Electronic Neural Networks, Continuous Synaptic Weights — The discrete weight neural elements described in the previous paragraph are best used in a convolution-like application (see the section below on the sensor processing networks) where the weights are fixed, and not adaptive. For applications that require adaption of the synapse weights (such as the system described in the next section), a completely analog approach, using neurons with continously adjustable synapse weights is preferable for reasons of circuit density and stability of the synaptic weight adaption process. Thus we have developed a current mode neural element which uses analog current multipliers to perform the synaptic weighting of the input currents.

A VLSI Self-Organizing Neural Network — One of the desirable properties of a neural network is its ability to adapt its synaptic weight according to some learning rule. We are investigating the implementation of a particular type of neural element, one in which the synapse weights are modified according to a Hebbian type of feedforward learning rule. It has been shown by Kammen and Yuille [3] that a feedforward network consisting of these types of neural elements performs self-organization in a manner similar to the development of neurons in mammalian visual cortex.

A single neural element, as implemented, contains 10 analog multiplier-based synapses, a current mode summing/sigmoid element, and a switched capacitor weight update circuit (one for each synapse). The weight update circuit that we have developed includes a current correlator and a leaky switched capacitor integrator. This weight modification circuit is what provides the learning and self-organizing behaviour of the neural element.

We have designed and laid out an integrated circuit in 2 micron CMOS double poly, double metal technology which contains 24 of the adaptive current mode neurons. This chip will be used to examine symmetry breaking and self-organization in

feedforward networks (work being done with Prof. Alan Yuille of Harvard and Dr. Dan Kammen of Caltech), and will also provide information on the dynamics of feedforward networks (work being done in conjunction with Prof. Robert Westervelt's research group, JSEP Unit 5). A test chip containing a single adaptive neuron is currently being fabricated by the MOSIS facility, and should be available in the latter part of the summer. The 24 neuron chip will be fabricated after information from the single neuron test cell is taken into consideration.

Integrated Sensor and Spatial Filter Arrays — We have taken the research begun in the previous JSEP grant cycle regarding the design and implementation of integrated sensor/spatial filter arrays to the implementation level. We have fabricated a 6×6 array of magnetic field sensors integrated with a current mode low pass filter followed by Laplacian (second derivative) filtering. This chip is currently being characterized. A second chip which uses circuitry closely related to the discrete neural elements described earlier, and which performs a spatial derivative operation on a 6×6 magnetic field sensor array is currently being fabricated and should be available for testing by mid-summer.

Tactile Sensor Implementation — Work on the magnetic field based tactile sensor described in the final report of the previous JSEP grant is continuing. We have completed the construction of external circuitry to perform sensor to sensor gain and offset compensation, and have installed the 32×32 magnetic field sensor array chip into a robotic gripper fingertip. We plan to produce improved versions of the magnetic sensor array chip that will have reduced gain and offset variation and higher attainable scan rates. This work is partially supported by NSF grant CDR–85–00108 in addition to the JSEP support.

Preliminary Endeavours

CMOS Active Sensor Chips — With an eye towards the application of the circuits described above, we have started examining integrated sensor/neural network circuitry for use in sensori-motor control systems. In these systems the signals from an array of sensors (typically tactile or optical sensors) are processed to provide a set of motor commands which execute a sensory-data-dependent action. For example such a system could process the output of a tactile sensor in such a way as to command a manipulator to trace along the edge of a surface. Such active sensing systems are potentially useful in constructing small autonomous systems wherein the centralized computational power available for sensori-motor processing is limited (cf., the artificial "insects" of Brooks [1]). We have just begun investigating these integrated active sensing systems, but have simulated a number of simple circuits that can be used in processing tactile data for computing the presence of contact and determining the desired direction of motion for aligning of fingertips with surface edges.

Temporally Modulated Neural Networks — A problem with neural networks arises when one tries to implement them in IC technology. Neural networks tend to have very high connectivity and cannot easily be embedded in low dimensional graphs. Therefore one has a problem in connecting neural elements on IC's which are planar processes and in which there are a limited number (3 or 4) of available wiring levels which can overlap.

To address this concern regarding neural networks we have begun investigating the design and implementation of neural networks for which the dynamics play an important role. We have built a software simulator for a axonal branching tree which acts as a temporal filter to decode temporally encoded pulse sequences [2]. Each branch point of the axonal tree either passes or blocks a pulse depending on a set of time constants and the previous history of the branch point. We plan to build

CMOS implementations of sensor processing arrays in which the sensory signals are temporally modulated and in which these axonal branching tree neural structures are used to demodulate the sensory signals. Using this approach we effectively trade off space for time and potentially achieve a denser packing of sensor and processing elements on a chip.

References:

1. Brooks, R., "A Robust Layered Control System for a Mobile Robot," MIT AI Lab. Technical Report, AIM-864 (1985).

2. Chang, S. H., Raymond, S. A., and Lettvin, J. Y., "Multiple Meaning in Single Visual Units," *Brain Behav. Evol.* **3**, 72–101 (1970).

3. Kammen, D. M., and Yuille, A. L., "Spontaneous Symmetry-breaking Energy Functions and the Emergence of Orientation Selective Cortical Cells," *Biological Cybernetics* **59**, 23–31 (1988).

ANNUAL REPORT OF

PUBLICATIONS/PATENTS/PRESENTATIONS/HONORS

a. Papers Submitted to Refereed Journals (and not yet published)

J. J. Clark, "Split Drain MOSFET Magnetic Sensor Arrays," *Sensors and Actuators* (accepted for publication).

b. Papers Published in Refereed Journals

J. J. Clark, "Singularity Theory and Phantom Edges in Scale Space," *IEEE Transactions on Pattern Analysis and Machine Intelligence*, Vol. 10, No. 5, Sept. 1988, pp. 720–727.

J. J. Clark, "Authenticating Edges Produced by Zero Crossing Algorithms," *IEEE Transactions on Pattern Analysis and Machine Intelligence*, Vol. 11, No. 1, Jan. 1989, pp. 43–57.

j. Graduate Students and Postdoctorals Supported Under the JSEP for the Year Ending 1 August October, 1989.

Mr. D. Friedman and Mr. T. L. Hwang

III.2 Decision and Control — Discrete Event Dynamic Systems Study. Y. C. Ho and D. D. Yao, Grant N00014–89–J–1023, Contracts ONR-N00014–86–K–0075, NSF-ESC–85–15449, NSF-CDR–85–001–08, and NSF-FCS–86–58157; Research Unit 10.

In 1988–89, Ho continued his research in Discrete Event Dynamics Systems (DEDS) and Perturbation Analysis (PA). These two acronyms have by now become accepted in the literature. Particularly noteworthy is the recognition by the National Science Foundation in their Guide to Programs 1989 of DEDS as a distinct research topic and the special issue devoted to DEDS by the Proceedings of IEEE which our group at Harvard helped edit and to which we contributed. Research in PA during 1988–89 concentrated on extending its applicability to more situations in which it was previously thought to be inapplicable. The principal techniques used are statistical equivalence and model representation. A DEDS can often be mathematically modeled in different but statistically equivalent representations. The simplest example is to use either a fair coin or a uniform random number generator to model 50–50 chance occurrence. A more elaborate example is the use of a single load-dependent server to represent a multiserver station. It turns out that such different representations can be effectively employed to extend the applicability of infinitesimal PA to

(i) multiclass M/G/1 servers

(ii) parallel simulation of Markov nonproduct-form queueing networks, and

(iii) G/G/m queues.

During the past year, David Yao has carried out the following:

(i) Developed the notion of *stochastic convexity* and studied its closure properties. This notion provides second-order optimality conditions for stochastic optimization algorithms (e.g., Robbins-Monro). These algorithms have recently received extensive research attention and applications, largely due to the development of

powerful sample-path gradient estimation techniques, such as *perturbation analysis*. A doctoral advisee of Yao, Kenneth Budka, has been working on stochastic optimization of stochastic networks with applications in flow control in communication systems. Independently, two doctoral advisees of Ho, Michael Fu and Jianqiang Hu, have found that stochastic convexity is also an essential property that ensures the sample-path gradient estimates obtained via perturbation analysis to be strongly consistent.

(ii) Applied polymatroid optimization techniques to solve scheduling control and/or load balancing problems in the Integrated Services Digital Network (ISDN) as well as distributed computer systems. Studied the stochastic monotonicity properties of circuit-switched communication networks (formulated as a stochastic knapsack problem). Studied modeling and analysis aspect of processor schedules in token ring Local Area Network (LAN).

(iii) Studied the scheduling control in *fluid networks*. A fluid network is a deterministic network model in which dynamic continuous flows are circulated and processed among a set of stations. A fluid network often captures the asymptotic behavior of a stochastic network via functional law of large numbers. The scheduling control of multi-class fluid networks can be systematically solved through a sequence of linear programs. The most encouraging fact is that in a single-server network, this solution procedure recovers the Gittins index set that solves the corresponding discrete queueing network model, widely known as Klimov's problem. This suggests that control policy derived from solving the fluid network model may also be very good (if not optimal) for the original queueing network (for which a direct approach to the control problem is in general intractable).

Professor Yao has resigned his Harvard appointment to accept a tenured position at Columbia University. Professor Ho will assist in the supervision of his students until their Ph.D. work is complete.

ANNUAL REPORT OF

PUBLICATIONS/PATENTS/PRESENTATIONS/HONORS

a. Papers Submitted to Refereed Journals (and not yet published)

M. Fu and J. Q. Hu, "Consistency of Infinitesimal Perturbation Analysis for the G1/G/m Queue," submitted to *European Journal of Operational Research.*

M. Fu "Convergence of a Stochastic Approximation Algorithm for the G1/G/1 Queue Using Infinitesimal Perturbation Analysis," submitted to *Journal of Optimization Theory and Applications.*

M. Fu and Y. C. Ho, "Using Perturbation Analysis for Gradient Estimation, Averaging, and Updating in a Stochastic Approximation Algorithm," *Proceedings of the Winter Simulation Conference*, 1988, pp. 509–517, to appear.

M. Fu, "On the Consistence of Second Derivative Perturbation Analysis Estimators for the M/G/1 Queue," to appear in *Applied Mathematics Letters.*

B. Zhang and Y. C. Ho, "Variance Reduction for Likelihood Ratio Methods," submitted to *28th CDC.*

B. Zhang and Y. C. Ho, "Likelihood Ratio Methods Using A-Segments," submitted to *Performance Evaluation.*

J. G. Shanthikumar and D. D. Yao, "Bivariate Characterization of Some Stochastic Order Relations," submitted to *Advances in Applied Probability.*

J. G. Shanthikumar and D. D. Yao, "Monotonicity and Concavity Properties in Cyclic Queueing Networks with Finite Buffers," in *Queuing Networks with Blocking* (eds. H. Perros and T. Altiok) (North Holland), to appear.

H. Chen and D. D. Yao, "Derivatives of the Expected Delay in G1/G/1 Queues," *Journal of Applied Probability*, to appear.

H. Chen and D. D. Yao, "Optimal Intensity Control of a Queueing System with State-Dependent Capacity Limits," *IEEE Transactions on Automatic Control*, accepted for publication.

K. W. Ross and D. D. Yao, "Optimal Load Balancing and Scheduling in a Distributed Computer System," submitted to *Journal of the Association for Computing Machinery.*

K. W. Ross and D. D. Yao, "Monotonicity Properties for the Stochastic Knapsack," submitted to *IEEE Transactions on Information Theory.*

J. G. Shanthikumar and D. D. Yao, "Spatiotemporal Convexity of Stochastic Processes and Applications," submitted to *Mathematics of Operations Research.*

L. Servi and D. D. Yao, "Bounds for Queueing Systems with Limited Service Schedules," *Performance Evaluation*, accepted for publication.

J. G. Shanthikumar and D. D. Yao, "Strong Stochastic Convexity: Closure Properties and Applications," submitted to *Advances in Applied Probability.*

b. Papers Published in Refereed Journals

Y. C. Ho (editor), Special Issue on the Dyanmics of Discrete Event Systems, *Proceedings of IEEE*, Jan. 1989.

Y. C. Ho, "Recent Developments in Perturbation Analysis," Proceedings of the IFAC Workshop on Decision Making in Manufacturing Automation, Sept. 1989.

J. G. Shanthikumar and D. D. Yao,"Stochastic Convexity and Its Applications in Parametric Optimization of Queueing Systems," *Proceedings of 27th IEEE Conference on Decision and Control*, Austin, TX, 1988, 657–662.

K. W. Ross and D. D. Yao, "Optimal Dyanamic Scheduling in Jackson Networks, *IEEE Transactions on Automatic Control*, **34**, 47–53 (1989).

g. Invited Presentations at Topical or Scientific/Technical Society Conferences

Y. C. Ho, 30 years of control, University of Rhode Island, June 3, 1988.

Y. C. Ho, Workshop on DEDS, American Control Conference, June 14, 1988.

Y. C. Ho, NSF Conference on DEDS, June 29, 1988.

Y. C. Ho, Symposium on Intelligent Control, August 25–26, 1988.

Y. C. Ho, Short Course on DEDS, University of Texas, Austin, October 24 to November 4, 1988.

Y. C. Ho, Polytechnic of Torino, Italy, November 22–27, 1988.

Y. C. Ho, Conference on Decision and Control, December 9, 1988.

Y. C. Ho, Rice University, December 10, 1988.

Y. C. Ho, Winter Simulation Conference, December 12, 1988.

Y. C. Ho, Carnegie-Mellon University, January 25, 1989.

Y. C. Ho, Washington University, St. Louis, January 26, 1989.

Y. C. Ho, University of Arizona, Tucson, AZ, January 28, 1989.

Y. C. Ho, Three lectures at University of Maryland, May, 1–6, 1989.

Y. C. Ho, SIAM Control in the 90's Conference, May 17, 1989.

D. D. Yao, ORSA/TIMS Annual Meeting, October, 1988.

D. D. Yao, Yale University, November, 1988.

D. D. Yao, Massachusetts Institute of Technology, November, 1988.

D. D. Yao, Bell Laboratories, February 1989.

D. D. Yao, NSF-IBM Presidential Young Investigators Conference, April 1989.

D. D. Yao, Computer and Information Sciences and Engineering ORSA/TIMS Annual Meeting, May, 1989.

i. Honors/Awards/Prizes

Y. C. Ho was given the 1989 IEEE field award for Control Science and Engineering.

Y. C. Ho was appointed Visiting Cockrell Family Regental Chair in Engineering at University of Texas.

j. Graduate Students and Postdoctorals Supported Under the JSEP for the Year Ending 1 October 1988.

Drs. S. Strickland, P. Q. Tang, B. Zang, Messrs. J. Feiger, M. Fu, J. Q. Hu, and L. Y. Shi.

IV. ELECTROMAGNETIC PHENOMENA

Personnel

Prof. T. T. Wu
Prof. R. W. P. King
Dr. J. M. Myers
Dr. H.-M. Shen
Mr. G. Fikioris
Mr. D. K. Freeman
Ms. M. Owens
Ms. B. H. Sandler

Research in the area of electromagnetic radiation is directed toward the solution of practical problems through the complete understanding of the underlying physical phenomena. This involves the coordinated application of modern analytical, numerical, and experimental techniques and the use of high-speed computers and precision instrumentation. Application is also made of modeling techniques and the principle of similitude. Most practically significant problems in the area are sufficiently complicated that extensive computation and measurement are often required to justify approximations that are usually necessary. Where possible, general formulas are obtained and verified experimentally so that the phenomenon under study can be understood physically in analytical form and not just as a set of numbers.

The researches are concerned primarily with the properties of antennas and arrays and of the electromagnetic fields they generate in various practically important environments that lead to difficult problems with complicated boundary conditions. Examples include dipoles, insulated antennas, traveling-wave antennas and arrays, crossed dipoles, and loops near the boundary between two media such as air and the earth or sea, or the oceanic crust and sea water; the properties of lateral electromagnetic waves; lateral waves and reflected waves in horizontally-layered media; the generation, propagation, and reception of lateral electromagnetic pulses; arrays

of antennas along curved lines; and solitary electromagnetic pulses with slow rates of decay.

IV.1 Analytical and Numerical Determination of the Fields of Antennas near an Interface Between Two Half-Spaces with Significantly Different Wave Numbers. T. T. Wu, R. W. P. King, B. H. Sandler, and M. Owens, Contract N00014-84-K-0465 and Grant N00014-89-J-1023; Research Unit 11.

Electromagnetic surface waves of a type known as *lateral waves* are excited along a boundary between two electrically different half-spaces by both vertical and horizontal electric dipoles located near or on that boundary. Beginning with the papers by Wu and King [1], [2], and King and Wu [3] for the horizontal dipole and by King [4] for the vertical dipole, the general integrals for the components of the electric and magnetic fields were integrated to obtain simple, accurate and continuous formulas valid over radial distances from very close to the source to infinity. These apply specifically to the field in Region 1 and along the boundary in Region 2, subject to the inequality $|k_1| \geq 3|k_2|$ where k_1 and k_2 are the wave numbers of the two half-spaces.

This early work was then extended to include the determination of integrated formulas for the field throughout Region 2 (the half-space in which the lateral wave travels) for both horizontal [5] and vertical [6] electric dipoles located near the boundary in Region 1. The field in Region 2 is shown to include an outward-traveling spherical wave and a lateral wave. The availability of integrated formulas for the field in Region 2 has permitted a detailed study of the properties of the lateral-wave part of the field, including the locus of the Poynting vector, the maximum depth of penetration of the lateral wave into Region 2, and the fraction of power associated with the lateral wave.

More recently, these results have been extended to obtain simple integrated

formulas for the complete electromagnetic field (not just the far field) at any point in the air (Region 2) when the dipole is at a height d also in the air [7]. Of particular interest in radio communication over the surface of the earth is the field at any point in Region 2 (air) when the dipole is on the surface of Region 1 (earth or sea). This field is completely and accurately given by the general formulas with $d = 0$. Using the large-argument approximation of the Fresnel-integral terms, simple expressions are also obtained for the complete far field of the unit vertical dipole on the surface of Region 2. During the current reporting period, a paper on this subject has been written and submitted for publication [8]. Graphs of the magnitude of $E_{2\Theta}(r_0, \Theta)$ for a unit vertical dipole for four different Regions 1 (salt water, lake water, wet earth, dry earth) show that the oscillations in the field patterns are due to interference between the combined direct and image fields and the surface-wave field—this is not confined to the boundary but extends a significant distance upward into the air. The oscillations decrease in amplitude with increasing conductivity σ_1; they disappear when Region 1 is a perfect conductor with $\sigma_1 = \infty$. The magnitude of $E_{2\Theta}(r_0, \pi/2)$ is due entirely to the lateral wave.

References:

1. T. T. Wu and R. W. P. King, "Lateral Waves: A New Formula and Interference Patterns," *Radio Science* **17**, 521–531 (1982).

2. T. T. Wu and R. W. P. King, "Lateral Waves: New Formulas for $E_{1\phi}$ and E_{1z}," *Radio Science* **17**, 532–538 (1982); Correction, **19**, 1422 (1984).

3. R. W. P. King and T. T. Wu, "Lateral Waves: Formulas for the Magnetic Field," *J. Appl. Phys.* **54**, 507–514 (1983); Erratum, **56**, 3365 (1984).

4. R. W. P. King, "New Formulas for the Electromagnetic Field of a Vertical Electric Dipole in a Dielectric or Conducting Half-Space near its Horizontal Interface," *J. Appl. Phys.* **53**, 8476–8482 (1982); Erratum, **56**, 3366 (1984).

5. R. W. P. King, M. Owens, and T. T. Wu, "Properties of Lateral Electromagnetic Fields and Their Application," *Radio Science* **21**, 13–23 (1986).

6. R. W. P. King, "Properties of the Lateral Electromagnetic Field of a Vertical

Dipole and Their Application," *IEEE Trans. Geosci. & Remote Sensing* **GE–24**, 813–825 (1986).

7. R. W. P. King, "Lateral Electromagnetic Surface Waves and Pulses," invited paper, presented at the Heinrich Hertz Symposium, Universität Karlsruhe, FRG, March 14 and 15, 1988.

8. R. W. P. King, "Electromagnetic Field of a Vertical Dipole Over an Imperfectly Conducting Half-Space," *Radio Science*, submitted for publication.

IV.2 Theoretical Study of Lateral-Wave Propagation in Horizontally-Layered Media. R. W. P. King, B. H. Sandler, and T. T. Wu, Contract N00014-84-K-0465 and Grant N00014-89-J-1023; Research Unit 11.

The theoretical work described in the preceding topic is concerned with the electromagnetic field generated by dipoles near the boundary between two homogeneous but electrically different half-spaces. Both half-spaces are assumed to be isotropic. In a more general form, one of the half-spaces is composed of a succession of n horizontally bounded layers each with arbitrary thickness and arbitrary wave number. Each layer is homogeneous and isotropic but the wave number is discontinuous across the boundaries. Below the n^{th} layer the rest of the half-space is homogeneous and isotropic to infinity. This layered model is used by geophysicists in the study of the oceanic crust. The general integrals for the electromagnetic field of a dipole in the one homogeneous, isotropic half-space separated from the second such half-space by the n horizontal layers of arbitrary electrical properties have been formulated, and from them simple integrated formulas have been obtained.

These general formulas have then been applied to a layered region with the properties of microstrip. In a recent paper [1], the electric field generated by a horizontal electric dipole on the air-substrate boundary of open microstrip has been calculated from the exact integrals subject to the inequalities $k_0^2 < |k_1^2| \ll |k_2^2|$, where k_0 is the wave number of air, k_1 the wave number of the dielectric substrate, and k_2 the wave number of the conducting base. It was shown that each component of the field consists of two parts: a lateral wave that travels in the air and a

direct wave that travels in the substrate. Since the two waves travel with different velocities, viz., $c = 3 \times 10^8$ m/sec in the air and $v = c\epsilon_{1r}^{-1/2}$ in the dielectric with the relative permittivity ϵ_{1r}, the superposition of the two must yield interference patterns. Such a pattern was shown in [1, Fig. 2] for an air-distilled water boundary when the water is a half-space. In a new paper [2], similar interference patterns are shown to exist in the microstrip. Calculations from the complete formulas in [1] for the components of the electric field tangent to the air-substrate boundary clearly show that sharp interference patterns occur in the vicinity of the radial distance where the lateral wave and the direct wave have equal magnitudes. At distances beyond the point of intersection, the lateral wave dominates.

The new paper [2] also investigates the field generated by the *pulse* excitation of a horizontal dipole on the air-substrate boundary of microstrip. Use is made of newly derived, explicit formulas for the transient electromagnetic field of a horizontal electric dipole on the boundary between two dielectric half-spaces when the dipole is excited by a Gaussian current pulse [3]. Relatively simple formulas are derived for the z- and ρ-components of the electric field on the surface of the dielectric. The coexistence of a lateral wave and a direct wave leads to a succession of two pulses with quite different shapes and rates of decrease in amplitude with distance. These differences are clarified. The significance of the lateral wave in providing strong long-range coupling among collinear elements in continuous-wave and pulse propagation along microstrip transmission lines is also demonstrated.

References:

1. R. W. P. King, "The Propagation of Signals Along a Three-Layered Region: Microstrip," *IEEE Trans. Microwave Theory & Tech.* **MTT-36**, 1080–1086 (1988).

2. R. W. P. King, "Lateral Electromagnetic Waves and Pulses on Open Microstrip," *IEEE Trans. Microwave Theory & Tech.*, accepted for publication.

3. R. W. P. King, "Lateral Electromagnetic Pulses Generated on a Plane Boundary Between Dielectrics by Vertical and Horizontal Dipole Sources with Gaussian Pulse Excitation," *Journal of Electromagnetic Waves and Applications*, accepted for publication.

IV.3 Lateral Electromagnetic Waves from a Horizontal Antenna for Remote Sensing in the Ocean. R. W. P. King, Contract N00014-84-K-0465 and Grant N00014-89-J-1023; Research Unit 11.

The method developed earlier [1], [2] for finding a buried metal cylinder in the earth can be adapted to the search for cylindrical metal objects like mines and submarines in the ocean or lying on the sea floor. Because salt water has quite different properties from earth, both the theoretical adaptation and the practical application of the method involve significant modifications that are scientifically interesting. These include the following: (a) The fluid nature of water makes it possible to locate and move both the transmitting and receiving antennas, not in the air, but in the same medium as the cylinder to be located. This greatly increases the magnitude of the receivable scattered signal and significantly reduces the possible interference by reflections from the ionosphere, because the transmission coefficient of a plane wave normally incident on the surface of the sea from the air is very small at the frequencies involved. (b) The much higher conductivity of the sea water compared to earth leads to a much greater complex wave number for electromagnetic waves. The associated wavelength is much shorter than that in the earth at the same frequency. It follows that a much lower frequency must be used in order to have the scattering cylinder with length $2h$ near resonance. Associated with the use of a lower frequency is a helpful decrease in the exponential attenuation of a traveling wave and a disadvantageous shift in the properties of lateral waves from those of the intermediate field with a radial decrease with distance of ρ^{-1} to the near field with a radial decrease of ρ^{-3}. Account is readily taken in the analysis of these important facts. A systematic study has been made [3] of the

several important factors involved in the development of a method for locating submerged submarines from measurements of the scattered electromagnetic field at the surface. These involve the properties of crossed antennas in the sea at very low frequencies and the circularly polarized lateral-wave fields they generate, as well as the field scattered by a submarine and a crossed receiving antenna to detect this. Representative calculations are made to illustrate the relative orders of magnitude of the dimensions and fields involved and the required sensitivity of a receiver.

References:

1. R. W. P. King, "Scattering of Lateral Waves by Buried or Submerged Objects. I. The Incident Lateral-Wave Field," *J. Appl. Phys.* **57**, 1453–1459 (1985).

2. R. W. P. King, "Scattering of Lateral Waves by Buried or Submerged Objects. II. The Electric Field on the Surface Above a Buried Insulated Wire," *J. Appl. Phys.* **57**, 1460–1472 (1985).

3. R. W. P. King, "Lateral Electromagnetic Waves from a Horizontal Antenna for Remote Sensing in the Ocean," *IEEE Trans. Antennas Propagat.*, accepted for publication.

IV.4 Lateral Electromagnetic Pulses Generated by Horizontal and Vertical Dipoles on the Boundary Between Two Dielectrics. T. T. Wu and R. W. P. King, Contract N00014-84-K-0465 and Grant N00014-89-J-1023; Research Unit 11.

In a recent paper [1] formulas are derived for the transient field generated by a vertical electric dipole on the boundary between air [Region 2; $k_2 = \omega(\mu_0\epsilon_0)^{1/2}$] and a dielectric half-space [Region 1; $k_1 = \omega(\mu_0\epsilon\epsilon_0)^{1/2}$] when excited by a Gaussian pulse. The time-domain formulas are obtained by Fourier transformation of the corresponding steady-state formulas. Since these are approximate in the sense that the permittivity of the dielectric is assumed to be large compared with that of air, the transient formulas derived from them do not include a second, much smaller pulse that travels in the dielectric and arrives much later than the main lateral pulse that travels in the air. This leaves some uncertainty about the accuracy of

the approximate transient formulas at and near the time of arrival of the second pulse.

A new paper [2] has been written to obtain the exact field so that this question can be clarified. Since an exact formula is available for the vertical component of the electric field when the vertical dipole is excited by a delta-function pulse [3], this can be applied to obtain the corresponding component of the transient field with Gaussian-pulse excitation. The resulting integral has been evaluated numerically and compared with the approximate field. The agreement is very good. The only differences are a somewhat more rounded minimum and somewhat sharper maximum in the exact pulse and the nonappearance of the relatively small second pulse in the approximate field.

The question about the second pulse that travels in the dielectric and arrives at a later time is completely resolved in the exact solution. The second pulse is seen to arrive at the predicted time, and to have a Gaussian shape with an amplitude that is very much smaller than that of the first pulse, as expected. An important insight gained from the approximate formulas is an explanation of the quite different shapes of the two pulses. The first pulse is dominated by the derivative of the Gaussian pulse with its $1/\rho$ amplitude factor. The Gaussian term has the amplitude factor $1/\rho^2$, so that it decays much more rapidly with increasing radial distance. Since the second pulse has the Gaussian shape, it must also be a $1/\rho^2$ term—but it is missing from the approximate formulas.

Since the transient field calculated by Fourier transformation of the approximate steady-state formulas gives accurate results for the vertical dipole except for the nonappearance of the small second pulse, the same should be true of the very similar field of the horizontal dipole on the boundary $z = 0$ in the dielectric. The corresponding approximate formulas are derived in [2] for the electric field of a horizontal dipole. It is seen that the transient field on the boundary surface generated

by a single Gaussian current pulse consists of two outward traveling pulses. One travels in the air with the velocity c, the second travels in the dielectric with the velocity $c\epsilon^{-1/2}$. Except close to the source, the dominant part of the pulse in air consists of the $1/\rho$ terms in $E_{2z}(\rho, \phi, 0; t)$ and $E_{2\rho}(\rho, \phi, 0; t)$. These have the form $2\tau' \exp(-\tau'^2)$ of the derivative of the Gaussian pulse $\exp(-\tau'^2)$. The dominant part of the pulse in the dielectric consists of the $1/\rho^2$ terms in all three components. The $1/\rho^3$ terms constitute the static field due to the charges left on the ends of the dipole. This field remains after both pulses have traveled to infinite distance.

References:

1. R. W. P. King, "Lateral Electromagnetic Pulses Generated by a Vertical Dipole on a Plane Boundary Between Dielectrics," *Journal of Electromagnetic Waves and Applications* **2**, 225–243 (1988).

2. R. W. P. King, "Lateral Electromagnetic Pulses Generated on a Plane Boundary Between Dielectrics by Vertical and Horizontal Dipole Sources with Gaussian Pulse Excitation," *Journal of Electromagnetic Waves and Applications*, accepted for publication.

3. T. T. Wu and R. W. P. King, "Lateral Electromagnetic Pulses Generated by a Vertical Dipole on the Boundary Between Two Dielectrics," *J. Appl. Phys.* **62**, 4345–4355 (1987).

IV.5 Lateral Electromagnetic Waves (Manuscript for Book). R. W. P. King, T. T. Wu, M. Owens, and B. H. Sandler, Contract N00014-84-K-0465 and Grant N00014-89-J-1023; Research Unit 11.

It has become a tradition in the publication of researches in the area of electromagnetic phenomena to periodically summarize and coordinate major segments in book form. Accordingly, a manuscript is in preparation which contains the results of current and past researches on lateral electromagnetic waves that have been supported in large part by the Joint Services Electronics Program. The book is entitled "Lateral Electromagnetic Waves: Theory and Applications to Communication, Geophysical Exploration, and Remote Sensing." It has been accepted for pub-

lication by Springer/Verlag Publishers. The chapter headings are: 1. Historical and Technical Overview of Electromagnetic Surface Waves; Introduction to Lateral Waves, 2. Electromagnetic Preliminaries, 3. The Electromagnetic Field of a Unit Vertical Electric Dipole in the Presence of a Plane Boundary, 4. Applications of the Theory of the Vertical Dipole Near The Boundary Between Two Half-Spaces, 5. The Electromagnetic Field of a Horizontal Electric Dipole in the Presence of a Plane Boundary, 6. Interference Patterns; Comparison of Approximate Formulas with General Integrals and Measurements, 7. Applications of the Theory of the Horizontal Dipole Near the Boundary Between Air and Earth or Sea, 8. The Measurement of the Conductivity of the Oceanic Lithosphere with a Horizontal Antenna as the Source, 9. Lateral Waves in a One-Dimensionally Anisotropic Half-Space, 10. The Propagation of Lateral Electromagnetic Waves in Air over Vertical Discontinuities, 11. The Horizontally Layered Half-Space, 12. The Three-Layer Problem for Sediment on the Oceanic Crust, 13. Lateral Electromagnetic Pulses Generated by Vertical Dipoles, 14. Approximate Formulas for Lateral Electromagnetic Pulses Generated by Vertical and Horizontal Electric Dipoles, 15. The Propagation of Signals Along a Three-Layered Region: Open Microstrip, 16. Antennas in Material Media Near Boundaries: The Bare Metal Dipole, 17. Antennas in Material Media Near Boundaries: The Terminated Insulated Antenna, 18. The Wave Antenna.

IV.6 Theoretical Study of Isolated and Coupled Strip Antennas. R. W. P. King, Contract N00014-84-K-00465 and Grant N00014-89-J-1023; Research Unit 11.

The properties of the isolated strip antenna of width $2w$ are usually obtained from those of the circular tubular antenna of radius a by an application of the well-known equivalence, $w = 2a$. The parameters of the strip transmission line with conductors of width $2w$ and separated by the distance $b = 2d$ have been obtained in the past by conformal transformation subject to the inequality $d \ll$

$2w$, where it is assumed that the thickness of the strip is small compared to the skin depth. In order to obtain a more accurate and comprehensive treatment, the integral equations for isolated and coupled strip antennas have been derived [1]. It is shown that the exact kernels of the integral equations for the current in a tubular antenna with length $2h$ and diameter $2a$ and for a strip antenna with length $2h$ and width $2w = 4a$ are identical. The integral equations for the two-element array and the N-element circular array of strip antennas are formulated. The equations are solved specifically for the closely spaced two-strip array, and the properties of the two-strip transmission line are obtained. The simpler cross-sectional geometry of coupled strip antennas with all currents confined to planes permits a more accurate solution that takes account of the cross-sectional distribution of current in mutual as well as self terms. Thus, mutual coupling among strips can be evaluated more accurately than among tubular cylinders. A solution is obtained for the coupled integral equations for two parallel strips with equal and opposite total currents when so closely spaced that they constitute a strip line. Accurate general formulas are obtained for the line constants of the strip line. These are compared with the corresponding ones for the transmission line consisting of two tubular conductors.

In a separate study, the characteristic impedance and the complex wave number, together with the associated series impedance and shunt admittance per unit length, have been derived [2] for a horizontal wire with radius a or a strip with width $2w = 4a$ over a two-layered region. This consists of a layer of dielectric with thickness l over a conducting or dielectric half-space with large permittivity. The properties of the wire as an antenna or transmission line are determined from those of the insulated antenna with a two-layered eccentric insulation. The theory is extended to the strip conductor with the help of a comparison of the tubular and strip conductors over a perfectly conducting half-space.

Possible applications of the results include long wave antennas erected (a) on

concrete or asphalt slabs over the earth, or (b) over swamps or shallow ponds, lakes or tidal basins. The theory also applies to horizontal dipoles over any two-layered region. The analysis resembles that of open-wire transmission lines in that radiation into the air is neglected in the determination of the wave number and characteristic impedance and, therefore, of the current distribution. This is an excellent approximation when the conducting wire or strip is located at small electrical distances from the dielectric-coated half-space. Once the current distribution is known in terms of its dependence on the electrical properties of the several media involved, the electromagnetic field can be calculated from the known field of a unit horizontal dipole over a three-layered region.

Although the new theory of the strip transmission line does not apply directly to open microstrip transmission lines because the conducting strip is located above and not on the dielectric substrate, it is nevertheless closely related to the quasi-TEM approximations used in microstrip theory. In addition, the new theory includes the losses in the conducting strip, the dielectric substrate, and the conducting ground plane. Since they are due primarily to skin effect, they are frequency-dependent and this frequency dependence is properly contained in the formulas for the wave number and the characteristic impedance. It is significant, in this connection, that the losses in microstrip at frequencies above 40 GHz are primarily due to skin effect in the two conductors.

References:

1. R. W. P. King and T. T. Wu, "An Accurate Analysis of Coupled Strip Antennas and of the Strip Transmission Line," *Radio Science* **24**, 27–34 (1989).

2. R. W. P. King, "Wire and Strip Conductors over a Dielectric-Coated Conducting or Dielectric Half-Space," *IEEE Trans. Microwave Theory & Tech.* **MTT-37**, 754–760 (1989).

IV.7 Theoretical Study of Electromagnetic Pulses with a Slow Rate of Decay. T. T. Wu, J. M. Myers, H. M. Shen, and R. W. P. King, Contract N00014-84-K-0465, Grant N00014-89-J-1023, Army LABCOM Contract DAAL02-86-K-0095, and DOE Grant DE-FG02-84ER40158; Research Unit 11.

The interesting possibility of generating electromagnetic pulses in such a manner that the energy associated with them decreases with distance r much more slowly than the usual r^{-2} is being investigated both theoretically (this topic) and experimentally (see Topic IV.8). Such pulses are conveniently referred to as electromagnetic (EM) missiles [1].

Till now, all of the wide variety of known missiles have shared the property of propagating in essentially straight lines. In two recent papers [2], [3], it is shown that an EM missile can follow a path that is strongly curved. It is known that a straight missile can be produced from a disk (or rectangle) over which a spatially uniform current distribution covers a broad spectrum of frequencies. In the hope of finding a curved missile, this configuration was adapted so that successive frequency components $\mathbf{J}_k(\mathbf{r})$ in the current distribution are defined not on one rectangle, but on a succession of rectangles, each at a different angle $\phi_*(k)$ about a common axis. The modified current distribution produces the same total radiated energy as does the unrotated distribution. Thus, by the known properties of the straight missile [1], this energy is finite if $0 < \epsilon < 1$. The expression derived for the time-integrated Poynting vector shows that, for $\epsilon < \frac{1}{2}$, the flux drops off more slowly than ρ^{-2}. Combining these two conditions, one sees that an electromagnetic missile is obtained for $0 < \epsilon < \frac{1}{2}$. A significant fraction of the total radiated energy is contained in a sector or wedge-shaped region near the curved path. This sector has a small thickness in the direction of the current and a small angle in the direction of the rotated normal vector.

A summarizing review of the theory of electromagnetic missiles, including a

lengthy discussion of the various known examples, has been written [4]. An analysis not previously presented is given of the effect on the received energy of an upper bound on the frequency spectrum of certain practical current generators. Conditions are stated which are sufficient to guarantee that the bound on the frequency spectrum has only a minor effect on the received energy. An earlier paper on the analysis of the circular cylindrical lens as an electromagnetic-missile launcher has been recently published [5].

During this reporting period, the theoretical investigation of electromagnetic missiles at off-axis field points and their properties for the case when the launcher is a circular current disk has been completed [6], [7]. The results indicate that the electromagnetic-missile effect extends beyond the cylindrical region defined by the radius of the disk. In particular, the analysis has shown that the electromagnetic missile has the following properties in addition to the slow decrease of the energy: (1) The electromagnetic missile propagates with a waveform that remains similar in shape but diminishes in size; the width of the pulse is compressed according to z^{-1} and its amplitude decreases according to $z^{-\epsilon+1/2}$. (2) The transverse distribution of energy around the axis is stable, i.e., when the longitudinal distance increases, the transverse pattern of the energy remains the same. This "plane-wave beam-like" property is different from continuous-wave (CW) radiation, in which the energy pattern is like that of a spherical wave. (3) The transverse energy pattern has a cusp on the axis. This property is also different from CW radiation. With CW, the radiation has a flat top on the axis of the main lobe. Although derived for the case of a current in a plane, these properties are also valid for other EM-missile launchers, such as the open-ended waveguide and the spherical lens. A comparison with measurements of the electric field at points on- and off-axis when transmitted from a parabolic dish or an open-ended circular waveguide is discussed under Topic IV.8.

A rigorous analysis of the V-conical antenna, designed as a feeding antenna for use in the experimental study of EM missiles, has been completed [8]. This is an angular antenna that consists of a pair of infinitely long, triangular metal plates bent around a cone. The antenna is found to be frequency-independent, to emit a pure spherical wave even in the near region, and to have a directional field pattern. These characteristics make it very suitable as a feeding antenna in the electromagnetic-missile experiment, where an efficient and uniform illumination for a lens or reflector is needed.

One of the major theoretical efforts during the current reporting period has been to determine how the distribution of the electric field on the aperture of a parabolic dish affects the behavior of the EM missile. After transforming the emitted fields from the V-conical antenna to the fields reflected by the parabolic dish, a simple but accurate formula for the aperture fields was obtained. This formula shows that the electric field on the aperture is quite *nonuniform*—which raises the question whether the two-term formula used in the analysis of the circular disk is still valid, since it is based on an assumed uniform distribution. With this formula for the field on the aperture, the radiated EM fields were evaluated and surprising preliminary results were obtained: The nonuniform distribution of the aperture field does not affect the EM missile on the axis, so that the two-term formula is still valid. Evidently this is another advantage of the V-conical antenna. Further investigation has determined that: (1) The radiation field depends only on the angular average of the distribution rather than on its details; (2) The angular-average function (AVF) depends on the field point on-axis or off-axis, as well as on the distribution of the source; (3) The on-axis AVF is found to be constant and equal to 1 for the V-conical antenna, but not for other feeding antennas; (4) The off-axis AVF for a nonuniform distribution is different from that for a uniform distribution; (5) If the spectrum of the exciting pulse goes to infinity, as frequently assumed in

theoretical analyses, the nonuniform distribution does not affect the rate of energy decay; (6) If the exciting pulse is a practical one, i.e., has a frequency cut-off, the distribution affects the rate of decay significantly; the more uniformly the field is distributed, the more slowly it decreases. After comparing the decay for different categories of distributions, it has been found that the optimum distribution is uniform. So far, it can be implemented only by the V-conical antenna with a reflector or a hyperboloidal lens.

Another type of nonuniform distribution being investigated currently is an array consisting of point sources. Strictly speaking, the energy radiated from such an array cannot decrease more slowly than $1/z^2$ since the decay parameter ϵ is constrained by the condition of finite total energy and, hence, must be greater than 1. However, for practical excitations where the frequency spectrum has a cut-off, the constraint that ϵ be greater than 1 does not necessarily apply. In other words, the energy radiated from the array may decrease slowly within a *certain region*. The preliminary numerical analysis has shown that: (1) The uniform-disk EM-missile launcher can be replaced by an array of point sources of the same size; (2) Depending on the cut-off frequency, there is a minimum number of elements N_0 and a minimum distance z_0 beyond which the energy from the array can decrease as slowly as the energy from a uniform disk of the same size; (3) The energy radiated from the array increases with the number N of the elements according to N^2; and (4) If the elements of the array are *patch sources* rather than point sources, under certain conditions involving N_0 and z_0 the energy radiated from the array can also achieve slow decay. Examples of patch sources include open waveguides, parabolic dishes, and lenses.

References:

1. T. T. Wu, "Electromagnetic Missiles," *J. Appl. Phys.* **57**, 2370–2373 (1985).

2. J. M. Myers, H.-M. Shen and T. T. Wu, "Curved Electromagnetic Missiles," *J. Appl. Phys.* **65**, 2604–2610 (1989).

3. J. M. Myers, H.-M. Shen and T. T. Wu, "Curved Electromagnetic Missiles," presented at the SPIE O-E/LASE'89 Conference held in Los Angeles, CA, January 15–20 (1989).

4. T. T. Wu, H.-M. Shen, and J. M. Myers, "A Review of Electromagnetic Missiles," presented at the SPIE O-E/LASE'89 Conference held in Los Angeles, CA, January 15–20 (1989).

5. T. T. Wu, R. W. P. King, and H.-M. Shen, "Circular Cylindrical Lens as a Line-Source Electromagnetic-Missile Launcher," *IEEE Trans. Antennas Propagat.* **AP-37**, 39–44 (1989).

6. H.-M. Shen and T. T. Wu, "The Transverse Energy Pattern of an Electromagnetic Missile from a Circular Current Disk," presented at the SPIE O-E/LASE'89 Conference held in Los Angeles, CA, January 15–20 (1989).

7. H.-M. Shen and T. T. Wu, "The Properties of the Electromagnetic Missile," *J. Appl. Phys.*, accepted for publication.

8. H.-M. Shen, R. W. P. King, and T. T. Wu, "V-Conical Antenna," *IEEE Trans. Antennas Propagat.* **AP-36**, 1519–1525 (1988).

IV.8 Experimental Study of Electromagnetic Pulses with a Slow Rate of Decay. H.-M. Shen, R. W. P. King, and T. T. Wu, Contract N00014-84-K-0465, Grant N00014-89-J-1023, and Army LABCOM Contract DAAL02-86-K-0095; Research Unit 11.

The purpose of the experiment is to demonstrate missile-like electromagnetic pulses. More specifically, this is a program to build and test devices capable of launching electromagnetic missiles. The program must measure the EMP accurately enough to confirm the slow decay of the energy and provide the means for improving the design of the EM-missile launcher. Because a missile-like electromagnetic pulse (EMP) involves transients with rise times under 100 picoseconds, the measurement of short pulses is essential.

The experiment consists of an electromagnetic-missile launcher fed by a voltage pulse generator that radiates an EMP. The pulse travels above the ground plane, is received by an EMP sensor, and then recorded by a sampling oscilloscope. The platform is a 51 × 16 square-foot metal ground plane supported by a 4-foot-high

wooden frame. The EM field is radiated, propagated, and received above the ground plane. Due to the image effect, the EM field above the ground plane is equivalent to that in free space.

In order to detect very short electromagnetic pulses under 100 picoseconds in width, a receiving antenna with a wide band from 0 to 14 GHz is needed. The usual short dipoles or monopoles do not provide both the required fidelity (bandwidth) and sensitivity. Two new EMP sensors—the L-antenna and the V-antenna—have been designed, analyzed and tested [1]. They are simple and inexpensive, and can detect the electromagnetic pulse with both high fidelity and sensitivity. An approximate analysis is given in [1] for better understanding and optimum design of the proposed EMP antennas. Compared to other sensors of the same height, the bandwidth of the new sensors is two times wider; compared to sensors of the same bandwidth, the sensitivity is two times higher for the L-antenna and eight times higher for the V-antenna. Another advantage of the new sensors over the short dipoles is that there is no need for an integration to restore the waveform of the incident field; the output waveform is very nearly proportional to that of the incident field. This is a great advantage in the data processing since the integration would introduce significant error due to the DC offset. In the experimental study of electromagnetic missiles, the pulse widths detected by these new sensors is only 6% wider than that of the incident EMP.

In order to emit an EM pulse with a spherical wave front, a special feeding antenna—the V-conical antenna—has been designed, analyzed and tested [2]. Such a V-conical antenna has the ability to emit a pure spherical wave. This is very important in order to obtain an "in phase" plane-wave front at the aperture of the dish. Other advantages include the fact that its structure is suitable for combining with a lens or reflector, and a theoretical analysis of its properties is feasible.

After adopting the newly designed transmitting antenna (V-conical antenna)

and receiving antenna (L-antenna), the entire system was found to work properly up to 10 GHz. The first set of data has already been reported [3]. The measurements were taken at 16 evenly spaced observation holes along the z-axis on the ground plane. The EM pulse launcher was a parabolic dish. During the current reporting period, measurements have been taken of the off-axis electromagnetic fields launched from the parabolic dish on the ground plane [4], [5]. The off-axis observation holes are located in the z direction at z = 13, 25, 37 and 49 feet. At each of these distances, there are five holes, with a 1-foot separation between them, e.g., x = 0, 1, ..., 4 ft. The measured data show that: (1) The waveform of the EM field on the axis radiated from a parabolic dish excited by a single impulse consists of two mutually opposite pulses; when the off-axis distance x increases, the two pulses move apart and their amplitudes decrease; (2) The energy decreases transversely beyond the cylindrical region defined by the radius of the parabolic dish; and (3) The transverse distribution of the energy is stable within z = 37 feet. Beyond this distance, the transverse distribution changes and spreads. An examination of the data indicates that the measured waveforms at different off-axis locations are comparable with those calculated from the theory. When the energy distributions are compared, however, the measured values appear to spread faster than their theoretical counterparts. This may be due to the mechanical error of the parabolic dish.

Measurements were then taken of the off-axis electric field from an open waveguide on the ground plane. The measured waveforms from the open waveguide are comparable to those measured from the parabolic dish, except for complications due to the presence of EM pulses reflected from the wall of the tube. The measurements show that the magnitude of the waveforms from the open waveguide has increased by only 6%, which is a smaller increase than predicted by the theory. This may be because the length of the waveguide is too short to establish a stable TE_{11} mode

inside the tube.

A Fourier analysis of the frequency spectra of EM missiles radiated from a parabolic dish has been completed and differences in the behavior of the measured spectra of the electric field as a function of the distance z observed. Below 3 GHz and within 25 ft, the spectrum decreases with distance as $1/z$; above 8 GHz and between 25 ft and 49 ft, the spectrum remains almost unchanged. Corresponding calculations using a two-term formula for the field of a circular aperture have been compared with the experimental data from three successive sets of measurements.

In order to improve the low-frequency response of the L-antenna, efforts have recently been directed toward eliminating the reflection from its open end. Replacing the horizontal wire with a series of resistors has succeeded in significantly reducing the reflected pulse; the fast-rise reflected impulse has been changed to a slowly decaying negative tail, the amplitude of which is only 10%. An analysis of the resistively tapered L-antenna is now in progress.

References:

1. H.-M. Shen, R. W. P. King, and T. T. Wu, "New Sensors for Measuring Very Short Electromagnetic Pulses," *IEEE Trans. Antennas Propagat.*, submitted for publication.

2. H.-M. Shen, R. W. P. King, and T. T. Wu, "V-Conical Antenna," *IEEE Trans. Antennas Propagat.* **AP-36**, 1519–1525 (1988).

3. H.-M. Shen, "Experimental Study of Electromagnetic Missiles," presented at the SPIE O-E/LASE'88 Conference held in Los Angeles, CA, January 10–17 (1988); reprinted in *Microwave and Particle Beam Sources and Propagation*, Vol. 873, Proceedings of SPIE, 338–346 (1988).

4. H.-M. Shen and T. T. Wu, "The Transverse Energy Pattern of an Electromagnetic Missile from a Circular Current Disk," presented at the SPIE O-E/LASE'89 Conference held in Los Angeles, CA, January 15–20 (1989).

5. H.-M. Shen and T. T. Wu, "The Properties of the Electromagnetic Missile," *J. Appl. Phys.*, accepted for publication.

IV.9 Properties of Closed Loops of Pseudodipoles. T. T. Wu and D. K. Freeman, Contract N00014-84-K-0465, Grant N00014-89-J-1023, Air Force Contract F19628-88-K-0024, and DOE Grant DE-FG02-84ER40158; Research Unit 11.

In order to obtain a general idea of how sensitively the behavior of a super-gain antenna is related to its parameters, a circular array comprised of the simplest elements—point sources or pseudodipoles—is under investigation. Information is being sought on the nature of the relation between the resonant frequency and the size of the array, the number of elements, and the spacing between elements. It was previously known that the infinite linear array admits real (zero-width) resonances and that the circular array admits resonances whose widths are exponentially small as the number N of pseudopotentials becomes large. Further investigations have shown that there is a one-to-one correspondence between these resonances and the frequencies at which the directivity of the field pattern is maximum. Narrow natural resonances have been determined with $N = 20$; the resonant field and directivities have been calculated asymptotically. The adjustment to resonance corresponds to the intersection of the forward and backward directivity peaks—which are slightly shifted in opposite directions. The sharpest resonance is for the $m = N/2$ phase sequence for which the field pattern consists of N sharp peaks symmetrically distributed around the circle. At self-resonance—when all elements are symmetrically excited—a unidirectional pattern requires a change from the circular to an egg shape.

Currently, efforts are being made to ascertain whether or not electromagnetic circular arrays of cylindrical dipoles exhibit similar phenomena. Motivated by the pseudopotential, a new formulation has been adopted which treats the self- and mutual-coupling terms in a symmetric manner. It has been shown that with this formulation the kernel of the integral equation determining the symmetric current components has an exponentially small imaginary part. This strongly suggests the

existence of narrow resonances, like those observed for the pseudopotential. Efforts are presently underway to solve the integral equation asymptotically for the resonant currents, the locations of the resonances, and the corresponding resonance widths.

IV.10 Superdirective Properties of Closed Loops of Parallel Coplanar Dipoles. T T. Wu, R. W. P. King, G. Fikioris, and B. H. Sandler, Contract N00014-84-K-0465, Grant N00014-89-J-1023, Air Force Contract F19628-88-K-0024, Army LABCOM Contract DAAL02-86-K-0095, and DOE Grant DE-FG02-84ER40158; Research Unit 11.

A review [1] of available data from numerous experimental and theoretical researches—many carried out over 25 years ago—combined with a very recent quantum-mechanical investigation [2], has led to new insights into the possibilities of closed loops of dipoles as highly directional arrays. The critical newly emphasized feature is the remarkable high-Q property of a correctly designed closed loop of coplanar dipoles when only one element is driven and all dimensions—the length of the elements, their cross-sectional size and shape, the number of elements, and the circumference of the closed loop—are correctly chosen.

As a first step in the investigation of resonance phenomena in large circular arrays, the two-term analysis of the N-element circular array developed by Mack [3] and applied by him to arrays with N up to 20 has been extended to $N = 40$ and $N = 80$ with element #1 driven and all others parasitic [4]. The self- and mutual admittances have been determined at resonant spacings d/λ when the elements have the *antiresonant* half-length $h = 0.4484\lambda$ and the radius $a = 0.007022\lambda$. The results when the circumference of the circle is near 4λ are very similar for $N = 20$, 40 and 80 and the associated values of $d/\lambda = 0.2$, 0.1 and 0.052. The magnitudes of the currents in the elements on the side of the circle opposite the driven element are comparable in magnitude to the current in that element. The magnitudes of the currents around the circle and their phases are consistent with the picture of two waves of current traveling around the circle in opposite directions from the driven

element and interfering on the far side to form a standing wave with currents in the elements almost in phase. The directive field pattern is that of a tapered broadside array (due to the standing-wave section) and a superimposed endfire pattern (due to the traveling-wave sections) that largely cancels one of the two main lobes of the broadside pattern. Arrays with other spacings such as $d/\lambda = 0.14$ with $N = 40$ have similarly directive patterns. On the other hand, a small change to $d/\lambda = 0.13$ leads to entirely different currents and field pattern.

The two-term theory of circular arrays as formulated in [3] has certain limitations: (1) When the different sequence admittances, $m = 0, 1, \cdots, N/2$, are calculated, the sequence conductances for m near $N/2$ are very small and *negative* instead of *positive*; (2) When the phase sequences are all superimposed to produce one driven and $N - 1$ parasitic elements, the term $\sin k(h - |z|)$ appears in the currents for these latter. This indicates the presence of equal and opposite concentrations of charge at $z = 0+$ and $z = 0-$. This is correct for the driven element, but not for the parasitic ones for which the currents must have a continuous zero slope at $z = 0$. A more accurate formulation for the distribution of current on the elements than that provided by the two-term theory used by Mack has been derived; it is particularly essential with closely coupled long elements. The new work is contained in two papers by King [5], [6] that introduce a new approach to the analysis of arrays with elements that include some that are very closely spaced and many that are far apart. Of particular importance is the separation of elements into two groups, the one closely coupled with a strong effect on the distributions and amplitudes of the currents, the other with a far-field-like interaction. It is shown that the defining criterion for close coupling is not $kb_{ij} \leq 1$ but $b_{ij} \leq h$, where b_{ij} is the distance between elements i and j, h is their half-length and $k = 2\pi/\lambda$. This means that electrically short elements can be much closer together without close-coupling effects than long elements. The new study also shows that for electrically short

elements the two-term approximation—which reduces to a shifted-cosine current in all parasitic elements—is an excellent approximation.

Another possibility being examined to improve the accuracy of the presently available methods of analysis is the more accurate definition of the effective distances between the currents in the elements than the conventional assumption that they are concentrated along the axes. In particular, the problem of the small negative phase-sequence conductances $G^{(m)}$ which occur in the two-term formulation of the circular array is under examination. $G^{(m)}$ is proportional to $P^{(m)}$, the total power supplied to and radiated by the circular array in the mth phase sequence. It has been found that $G^{(m)}$ and $P^{(m)}$ depend critically on the "effective distance" $\bar{b}_j$ from dipole #1 to dipole #j entering the integral equation. Until now, the distance c_j from center to center has been used. The problem is three-dimensional; the actual distance b_j is the distance between two cylindrical surfaces and is a function of two angles. A relation giving $P^{(m)}$ in terms of the imaginary part of the kernel $K^{(m)}(z - z')$ has been derived. By demanding that $P^{(m)} > 0$, an inequality has been found which $\mathrm{Im}\{K^{(m)}(0)\}$ must satisfy. This inequality is a restriction on the $\bar{b}_j$'s. If c_j is used as the effective distance, then this inequality is found by computation not to be satisfied in many cases. In these cases, N is large, m is close to $N/2$ and the spacing is small, so that $P^{(m)}$ and $\mathrm{Im}\{K^{(m)}\}$ are very small and extremely sensitive to slight perturbations in the $\bar{b}_j$'s. By approximating the actual distance b_j, an effective distance is found that satisfies the inequality for all cases in which c_j does not. This $\bar{b}_j$ is larger than c_j and is a simple function of c_j and a. However, it is not certain that this newly determined effective distance is the correct one. The fact that the inequality is satisfied is simply a good indication.

An accurate analysis of the current near the open ends of a center-driven dipole has also been carried out [7], [8] as a necessary improvement on the trigonometric functions used to represent current distributions especially in long driven elements.

The three-term solution [9] is simple and gives a rather good approximation of the current over the length of the antenna except near the open end. An analysis of the current and charge distributions near the end of a tubular antenna using the Wiener-Hopf solution has shown that it is possible to derive accurate expressions for the current and charge near the end of a tubular antenna. The solution for the current near the end of the antenna is found to be a *universal* formula; i.e., when the frequency or length is changed, the relative distribution near the end remains the same. This is described in more detail under Topic IV.11.

References:

1. R. W. P. King, "Supergain Antennas and the Yagi and Circular Arrays," *IEEE Trans. Antennas Propagat.* **AP-37**, 178–186 (1989).

2. A. Grossmann and T. T. Wu, "A Class of Potentials with Extremely Narrow Resonances," *Chinese Jour. Phys.* **25**, 129–139 (1987).

3. R. W. P. King, R. B. Mack, and S. S. Sandler, *Arrays of Cylindrical Dipoles*, Chapter IV, Cambridge Univ. Press (1968).

4. "Developmental Study of Electromagnetic Missiles," Annual Progress Report No. 3, Army LABCOM Contract DAAL02-86-K-0095, Gordon McKay Laboratory, Harvard University (1989).

5. R. W. P. King, "Electric Fields and Vector Potentials of Thin Cylindrical Antennas," *IEEE Trans. Antennas Propagat.*, submitted for publication.

6. R. W. P. King, "The Large Circular Array with One Element Driven," *IEEE Trans. Antennas Propagat.*, submitted for publication.

7. H.-M. Shen and T. T. Wu, "The Universal Current Distribution Near the End of a Tubular Antenna," *J. Math. Phys.*, submitted for publication.

8. H.-M. Shen, R. W. P. King, and T. T. Wu, "The Combination of the Universal End-Current and the Three-Term Current on a Tubular Antenna," *IEEE Trans. Antennas Propagat.*, submitted for publication.

9. R. W. P. King and T. T. Wu, "Currents, Charges and Near Fields of Cylindrical Antennas," *J. Research NBS, Radio Science* **69D**, 429–446 (1965).

IV.11 Asymptotic Solution for the Charge and Current Near the Open End of a Linear Tubular Antenna. H.-M. Shen, T. T. Wu, and R. W. P. King, Contract N00014-84-K-0465, Grant N00014-89-J-1023, Army LABCOM Contract DAAL02-86-K-0095, and Air Force Contract F19628-88-K-0024; Research Unit 11.

Since the dipole antenna is one of the most useful forms of antenna, it has been analyzed extensively for more than half a century. Most of these analyses have dealt with the case where the radius of the dipole is small. In such cases, since the vector potential on the surface of the dipole is roughly proportional to the current, its distribution obtained theoretically is approximately sinusoidal or, more generally, a sum of several sinusoidal terms. This traveling-wave-like solution is mainly caused by the aspect of electromagnetic induction. There is, however, another aspect of this problem of the current distributions on the dipole antenna. Coulomb repulsion between charges of the same sign is always present. This repulsion leads to a larger charge density near the end of the rod than at the center. For the dipole antenna, this Coulomb repulsion leads to the result that the charge density and, hence, also the current cannot be described naturally and accurately as a sum of sinusoidal terms. This effect is most pronounced near the ends of the antenna; it is the subject of a new paper [1].

The basic idea of the paper is to use the Wiener-Hopf procedure of solving integral equations. This is intimately related to the observation that, except possibly for an overall constant, the current distribution near one end of a dipole antenna is approximately independent of the details near the other end. First, the problem of the current distribution near the end of the center-driven dipole antenna, where Coulomb repulsion is most pronounced, is formulated in terms of a Wiener-Hopf integral equation, which is then solved exactly. This exact solution is then evaluated approximately using the fact that the radius of the dipole antenna is small. This last step is technically complicated. Much effort has been directed toward changing the contours of the integration to improve the convergence. It is found

that the expression obtained for the current from the inverse Fourier transform is a *universal* formula in which no parameter other than the radius is involved; i.e., the relative distributions of charge and current are independent of the length of the antenna and the frequency of operation. This means that within the range of about a quarter-wavelength, the repulsion effect dominates the distributions of charge and current, so that these are significantly different from sinusoidal distributions which are the solutions from approximate theories.

With this newly derived universal formula for the current near the end of a tubular antenna, it is possible to improve the current distribution obtained from the approximate three-term solution [2]. In a second paper [3], the current near the end of the tube is represented by the universal formula derived in [1], the currents on the other parts of the antenna by the three-term solution. The currents and charges obtained from the two formulations are then matched at the junction. When the combined solution is compared with experimental results, it is seen that the currents at the end as well as the driving-point admittance have been improved significantly.

References:

1. H.-M. Shen and T. T. Wu, "The Universal Current Distribution Near the End of a Tubular Antenna," *J. Math. Phys.*, submitted for publication.

2. R. W. P. King and T. T. Wu, "Currents, Charges and Near Fields of Cylindrical Antennas," *J. Research NBS, Radio Science* **69D**, 429–446 (1965).

3. H.-M. Shen, R. W. P. King, and T. T. Wu, "The Combination of the Universal End-Current and the Three-Term Current on a Tubular Antenna," *IEEE Trans. Antennas Propagat.*, submitted for publication.

IV.12 Closed Loops of Parallel Coplanar Dipoles—Electrically Short Elements. T. T. Wu, R. W. P. King, and G. Fikioris, Contract N00014-84-K-0465, Grant N00014-89-J-1023, and Air Force Contract F19628-88-K-0024; Research Unit 11.

The first attempt to extend the analysis of large circular arrays to short lengths—specifically to the length $2h/\lambda = 0.36$ predicted for minimum loss [1, Fig. 5]—was not successful; no sharp resonances occurred. When the thickness of the elements was later increased from $a/\lambda = 0.007022$ to $a/\lambda = 0.028$, the results were startlingly different. The thicker array displays a remarkable set of sharp resonances. Investigation shows that each resonance corresponds to a particular dominant phase-sequence conductance $G^{(m)}$ in the sum over the $N/2$ phase sequences that determine the $N/2$ different currents. A preliminary study of the self- and mutual admittances (normalized currents) and far-field patterns of some of the phase sequences in arrays of 60, 72 and 90 elements has disclosed a remarkable set of properties that require a systematic investigation.

The $m = 10$ resonance with $N = 60$ is particularly interesting. The currents in the 60 elements form 20 *triplets* or groups of three, viz., 3-4-5, 6-7-8, ..., 60-1-2. The currents in the three elements in each group are almost in phase; the phase difference between the central elements in adjacent triplets is exactly 180°. The magnitude of the current in each central element is about double that in the adjacent two and very nearly equal to that in the central elements of the other triplets. The single exception is the driven element #1 which carries a current twice as large. The far-field power pattern consists of 20 sharp peaks between 20 nulls. The peaks occur in the directions of the central elements 1, 4, 7, ..., of the 20 triplets. The larger current in the driven element and the lack of exact equality in the phases of the currents in each triplet represent a rotational asymmetry with more power radiated in the backward direction. The resonance with triplets occurs with the particular resonant spacing near $d/\lambda = 0.132$ and with the dominant phase

sequence $m = (1/3) \cdot (N/2)$. There are $N/3$ nulls and $N/3$ sharp peaks in the field pattern provided the divisions yield integers. This general rule has been verified with $N = 60$ and $N = 90$. Thus, with $N = 90$ resonance occurs with $d/\lambda = 0.1328$, $m = 15$, $N/3 = 30$ nulls and peaks.

For the $m = 9$ resonance with $N = 72$, $m = 9 = (1/4) \cdot (72/2)$ suggests a subdivision into quadruplets with $(72/4) = 18$ nulls and 18 sharp peaks in the field pattern. The magnitudes and phases of the normalized currents in the elements are separated into 18 groups of triplets (4-5-6, 8-9-10, 12-13-14, ..., 72-1-2) with large currents and 18 singlets (3, 7, 11, ..., 71) with very small currents. The central elements of the triplets have the largest and almost equal currents. They differ in phase from one group of three to the next group of three by 180°. However, these groups of three are not adjacent but separated by the singlets. These have small currents and phases that differ by exactly 90° from the central elements of the adjacent triplets. The 18 peaks in the field pattern are determined by the 18 triplets. The deep minima (nulls) lie along the directions of the singlets which contribute little to the field.

The $m = 18$ resonance for $N = 72$ occurs at $d/\lambda = 0.2166$; $m = 18 = (1/2) \cdot (72/2)$ suggests doublets, $N/2 = 36$ peaks and 36 nulls. The magnitudes and phases of the normalized currents are clearly divided between two groups of 36 elements, the odd-numbered elements (1, 3, ..., 71) with large currents and the even-numbered elements (2, 4, ..., 72) with small currents. The phase difference from element to element within each group is 180°; from element to adjacent element it is 90°. Thus, each group is in the approximately neutral plane of the other. The field pattern has 36 peaks in the directions of the odd elements and 36 minima in the directions of the even elements.

In order to generate singlets, it is necessary that $m = N/2$. With $N = 90$, $m = 45$. The associated resonance peak is extremely sharp. It occurs at $d/\lambda =$

0.437432095 and the self-conductance $G_{1,1}$ has the very large value 3.256 Amp/V. (The corresponding value for $m = 10$ with $N = 60$ is 24 mA/V.) The self- and mutual conductances of all of the elements alternate between equal and very large positive and negative values. The associated susceptances are very small compared to the conductances, and the self-susceptance $B_{1,1}$ of the driven element #1 is very close to zero. This means that the driving-point impedance of the entire array at the terminals of element #1 *is a pure resistance* near 0.3 Ohm. The magnitudes of the normalized currents range from 3.255 Amp for the driven element to 3.235 Amp in element 45. The associated phases are alternately 0° and 180°. The far-field power pattern consists of 90 nulls between 90 very sharp spikes.

The successful confirmation of the existence of extremely sharp resonances in a circular array of 90 elements with the predicted minimum-insertion-loss length lays the foundation for a comprehensive study of the general principles involved and of the roles played by the several parameters.

Reference:

1. R. W. P. King, "Supergain Antennas and the Yagi and Circular Arrays," *IEEE Trans. Antennas Propagat.* **AP-37**, 178–186 (1989).

ANNUAL REPORT OF

PUBLICATIONS/PATENTS/PRESENTATIONS/HONORS

a. Papers Submitted to Refereed Journals (and not yet published)

R. W. P. King, "Lateral Electromagnetic Pulses Generated on a Plane Boundary Between Dielectrics by Vertical and Horizontal Dipole Sources with Gaussian Pulse Excitation," *Journal of Electromagnetic Waves & Applications* (accepted).

R. W. P. King, "Lateral Electromagnetic Waves from a Horizontal Antenna for Remote Sensing in the Ocean," *IEEE Trans. Antennas Propagat.* (accepted).

R. W. P. King, "Lateral Electromagnetic Waves and Pulses on Open Microstrip," *IEEE Trans. Microwave Theory & Tech.* (accepted).

H.-M. Shen, R. W. P. King, and T. T. Wu, "New Sensors for Measuring Very Short Electromagnetic Pulses," *IEEE Trans. Antennas Propagat.* (Partial support from Army LABCOM Contract DAAL02-86-K-0095.)

H.-M. Shen and T. T. Wu, "The Universal Current Distribution Near the End of a Tubular Antenna," *J. Math. Phys.* (Partial support from Army LABCOM Contract DAAL02-86-K-0095 and Air Force Contract F19628-88-K-0024.)

H.-M. Shen, R. W. P. King, and T. T. Wu, "The Combination of the Universal End-Current and the Three-Term Current on a Tubular Antenna," *IEEE Trans. Antennas Propagat.* (Partial support from Army LABCOM Contract DAAL02-86-K-0095 and Air Force Contract F19628-88-K-0024.)

R. W. P. King, "Electric Fields and Vector Potentials of Thin Cylindrical Antennas," *IEEE Trans. Antennas Propagat.* (Partial support from Air Force Contract F19628-88-K-0024.)

R. W. P. King, "The Large Circular Array with One Element Driven," *IEEE Trans. Antennas Propagat.* (Partial support from Air Force Contract F19628-88-K-0024.)

b. Papers Published in Refereed Journals

T. T. Wu, R. W. P. King, and H.-M. Shen, "Circular Cylindrical Lens as a Line-Source Electromagnetic-Missile Launcher," *IEEE Trans. Antennas Propagat.* **AP-37**, 39–44 (1989). (Partial support from Army LABCOM Contract DAAL02-86-K-0095.)

R. W. P. King, "Supergain Antennas and the Yagi and Circular Arrays," *IEEE Trans. Antennas Propagat.* **AP-37**, 178–186 (1989). (Partial support from Army LABCOM Contract DAAL02-86-K-0095 and Air Force Contract F19628-88-K-0024.)

H.-M. Shen, R. W. P. King, and T. T. Wu, "V-Conical Antenna," *IEEE Trans. Antennas Propagat.* **AP-36**, 1519–1525 (1989). (Partial support from Army LABCOM Contract DAAL02-86-K-0095.)

R. W. P. King and T. T. Wu, "An Analysis of Coupled Strip Antennas and of the Strip Transmission Line," *Radio Science* **24**, 27–34 (1989).

R. W. P. King, "Wire and Strip Conductors over a Dielectric-Coated Conducting or Dielectric Half-Space," *IEEE Trans. Microwave Theory & Tech.* **MTT-37**, 754–760 (1989).

J. M. Myers, H.-M. Shen, T. T. Wu, and H. E. Brandt, "Curved Electromagnetic Missiles," *J. Appl. Phys.* **65**, 2604–2610 (1989). (Partial support from Army LABCOM Contract DAAL02-86-K-0095.)

h. Contributed Presentations at Topical or Scientific/Technical Society Conferences

T. T. Wu, H.-M. Shen, and J. M. Myers, "A Review of Electromagnetic Missiles," presented at the SPIE O-E/LASE'89 Conference held in Los Angeles, CA, January 15–20 (1989).

J. M. Myers, H.-M. Shen and T. T. Wu, "Curved Electromagnetic Missiles," presented at the SPIE O-E/LASE'89 Conference held in Los Angeles, CA, January 15–20 (1989).

H.-M. Shen and T. T. Wu, "The Transverse Energy Pattern of an Electromagnetic Missile from a Circular Current Disk," presented at the SPIE O-E/LASE'89 Conference held in Los Angeles, CA, January 15–20 (1989).

j. Graduate Students and Post-Doctorals Supported under the JSEP for the Year Ending 31 July 1989

Dr. J. M. Myers, Dr. H.-M. Shen, Mr. G. Fikioris, Mr. D. K. Freeman.

V. SIGNIFICANT ACCOMPLISHMENTS REPORT

V.1 Harmonic Generation in High-Temperature Superconductors.

L. Ji, C. J. Lobb, and M. Tinkham; Research Unit 4, SOLID STATE ELECTRONICS.

Because of the highly nonlinear electrodynamic response of type-II superconductors to applied magnetic fields, the magnetization induced by a sinusoidal applied field contains a rich spectrum of harmonics of the drive frequency. Recently we and several other groups have applied this harmonic-analysis approach to study the nonlinear response of the high temperature superconductors, stimulated by the early work of Jeffries *et al.* [1]. The experimental work has shown that even harmonics are seen in addition to the usual odd ones if a dc field is present in addition to the ac probe field (thus breaking the symmetry), and it has revealed a rather complex and interesting dependence of the various harmonics on the strength of the ac and dc fields, on the temperature, and on sample quality. Jeffries *et al.*, interpreted their data in terms of a model of postulated current loops in the material interrupted by Josephson junction couplings between grains. Although this model could explain some of the data, it seemed rather *ad hoc*, and could not explain all aspects of the data in a consistent way. We have developed an alternative model, based on the "critical state" model introduced many years ago by Bean [2] to describe the irreversible magnetization of type-II superconductors, and find that it provides a much more natural explanation of all observed features, without requiring any *ad hoc* assumptions.

In the critical state, the superconducting material attempts to screen its interior from changing external fields H by carrying its critical current density as a screening current to a sufficient depth to screen the external change in field. As a

consequence, the larger the amplitude of the changing field, the deeper the penetration. A characteristic field parameter $H^* \sim DJ_c$ is the value of H at which field penetrates all the way to the center of a slab of thickness D. [This stands in sharp contrast with the *linear* response described by the London penetration depth, which is independent of field strength, and microscopic ($\sim$ 1000 Å) in magnitude.] In his original work, Bean assumed that the critical current density J_c was a constant, independent of H, leading to a linear screening profile for the internal flux density. He derived results for the amplitude of the harmonics, finding only odd harmonics, with amplitude increasing as H_{ac}^2 for $H_{ac} < H^*$, saturating at $H_{ac} \approx 4H^*$. With J_c taken as constant, the presence of H_{dc} has no effect; in particular, it produces no even harmonics.

The key step made by graduate student Li Ji to move this subject forward is to recognize the need to generalize the Bean model analysis to include a *field-dependent* critical current density $J_c(H)$. As an example, we have used the Anderson-Kim [3] model, which assumes a constant pinning force density, so that J_c varies *inversely* with the local magnetic field strength. This leads to parabolic rather than linear flux screening profiles, which modifies the quantitative results. More importantly, it brings in the symmetry-breaking effect of a dc magnetic field, since the *absolute value* of the field (and hence J_c) is no longer the same on alternate half-cycles of the drive field. We have worked out analytic results for $M(t)$ and also for the harmonic Fourier components, for comparison with experimental data. For example, Figure V.1 shows the predicted dependence on H_{dc}/H_{ac} of representative harmonic amplitudes. Note that the even harmonics show a sharp minimum (really zero) amplitude at $H_{dc} = 0$, and both odd and even harmonic amplitudes oscillate with a period that scales with $1/n$, where n is the harmonic number.

The comparison of this model with experimental data is complicated by the fact that the simple Anderson-Kim approximation that $J_c \sim 1/H$ leads to the

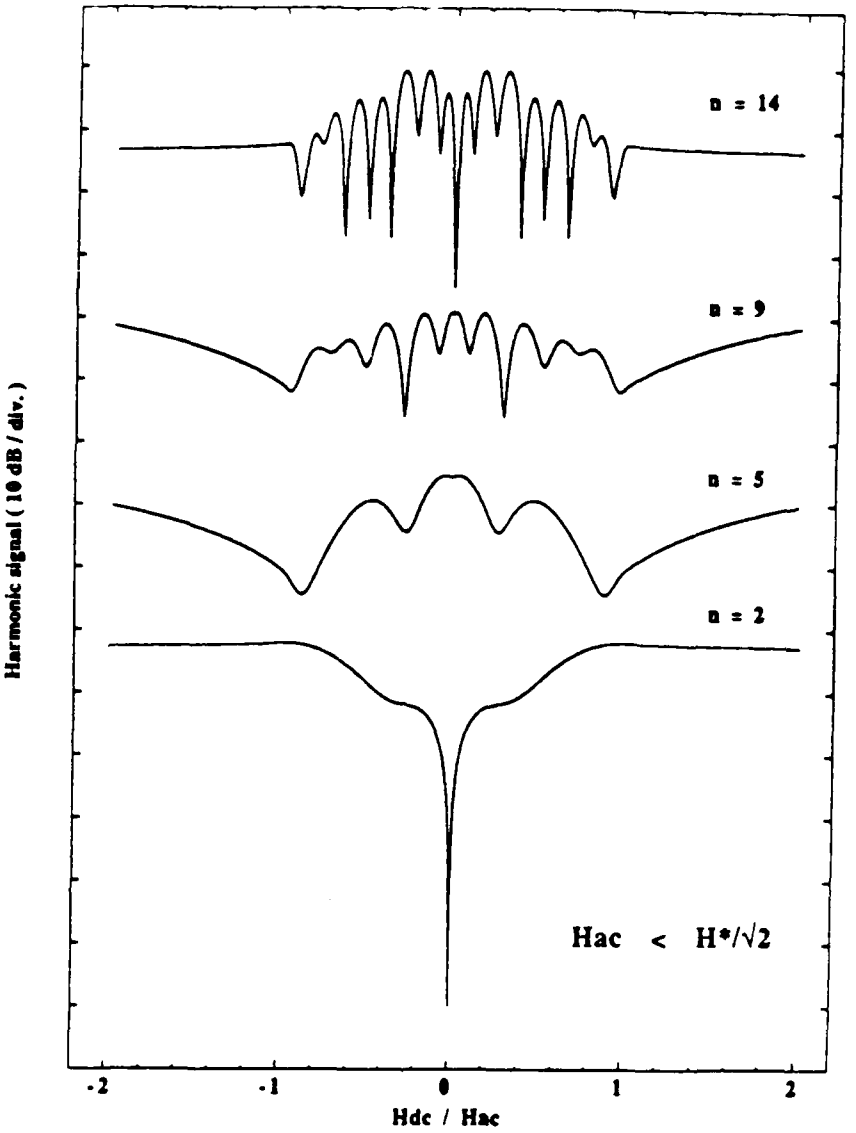

Fig. V.1. Harmonic signal amplitude calculated numerically from the Anderson-Kim model as a function of applied dc field for various harmonic number n. The form of these curves holds so long as $H_{ac} < H^*/\sqrt{2}$.

nonphysical result of $J_c = \infty$ for $H = 0$. This is usually cut off by introducing a parameter H_μ such that $J_c \sim (H + H_\mu)^{-1}$, but this makes the analysis of harmonic content mathematically unwieldy. Hence we [4] have concentrated on two limiting approximations: The Bean model, J_c = const. for H small or nearly constant; and the Anderson-Kim model $J_c \sim 1/H$ for large H; with a crossover in between. For example, in Figure V.2 we plot our experiment data for 3rd harmonic amplitude *vs.* H_{ac}, which demonstrates the crossover at about

3 Oe from the proportionality to H_{ac}^2 at low amplitudes, where the Bean model is more appropriate, to the H_{ac}^3 dependence predicted by the Anderson-Kim model appropriate at higher amplitudes.

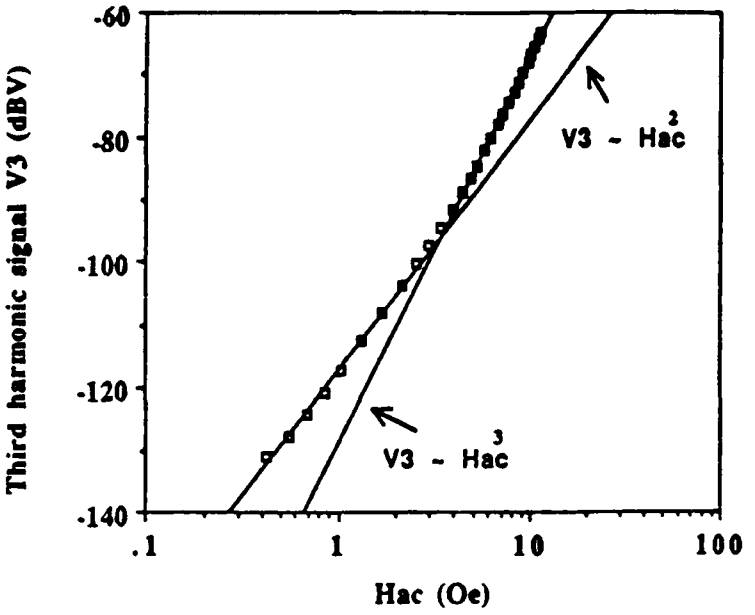

Fig. V.2. Third harmonic signal measured using bulk YBCO, for $H_{ac} << H^*$, showing transition from Bean regime (Signal $\sim H_{ac}^2$) to the Anderson-Kim regime (Signal $\sim H_{ac}^3$).

Our work to date has involved only kHz frequencies, where the response of the superconductors is essentially quasistatic. We plan to extend these experiments up to higher frequencies, to study the effect of relaxation processes immediately following field changes.

References:

1. C. D. Jeffries *et al.*, *Phys. Rev.* **B37**, 9840 (1988).
2. C. P. Bean, *Phys. Rev. Lett.* **8**, 250 (1962); *Revs. Mod. Phys.* **36**, 31 (1964).
3. P. W. Anderson and Y. B. Kim, *Revs. Mod. Phys.* **36**, 39 (1964).

4. L. Ji, R. H. Sohn, G. C. Spalding, C. J. Lobb, and M. Tinkham, *Phys. Rev.* **B**, submitted.

V.2 Resonant Closed Loops of Dipoles. T. T. Wu, R. W. P. King, and G. Fikioris; Research Unit 11, ELECTROMAGNETIC PHENOMENA,

Resonant circuits have played a major role in electrical technology and from simple tank circuits to cavity resonators they are well understood. A novel exception with remarkable properties has suddenly emerged: the closed loop of coplanar parallel dipoles [1]. In experimental research supported by the U.S. Air Force in the early 1960's [2], it was demonstrated that a correctly designed linear or semicircular array of coplanar parallel cylinders has unusual low-loss properties as a transmission line. At the same time, an extensive investigation [3], [4] of the circular array of coplanar parallel dipoles supported by the Joint Services disclosed the existence of sharp resonances in 20-element arrays of which only one was driven. In 1987 it was shown from a quantum-mechanical analogy [5] that closed loops of coplanar dipoles must have extremely sharp resonances. It was suggested that such loops could be proportioned to provide superdirective field patterns.

Extensive theoretical studies combined with numerical calculations during the past year have succeeded in determining some of the basic conditions that lead to a whole series of sharp resonances. These correspond to a variety of current distributions with a remarkable range of properties. For example, a circular array of 90 elements with the length $2h = 0.36\lambda$ and equally spaced at a very precisely defined distance near 0.437λ with only element #1 driven has the following properties: The currents in all elements have the same magnitude, *viz.*, 3.2 Ampere for each volt applied to the terminals of element #1; the phases of odd elements are 0, of the even elements 180°. The driving-point impedance of this very high-Q circuit is a *pure resistance* of 0.3 Ohms. The field pattern consists of 90 nulls between 90 very sharp

peaks in which the electric field has equal amplitudes and changes in phase by 180° from peak to adjacent peak. A small change in spacing to another resonance merely reverses the phases in the elements on one side of the array with no change on the side with the driven element at its center. The peaks in the forward and backward directions of the field pattern are greatly reduced, those in the lateral directions left unchanged. A shift in spacing to a third resonance, reduces the number of nulls and peaks to 30 by having groups of three elements in phase and 180° out of phase with the next group of three — still with only one element driven.

It is hoped that by changes in shape from the circle to an oval or egg shape similar resonances can be found that generate field patterns in which all the sharp peaks are small, except one very large one, so that a highly directive array is obtained.

References:

1. R. W. P. King "Supergain Antennas and the Yagi and Circular Arrays," *IEEE Trans. Antennas Propagat.* **AP-37**, 178–186 (1989).

2. J. Shefer, "Periodic Cylinder Arrays as Transmission Lines," Cruft Laboratory Scientific Report No. 14, Contract AF19(604)-4118, Harvard University (1962).

3. R. B. Mack, "A Study of Circular Arrays. 2. Self and Mutual Admittances," Cruft Laboratory Technical Report No. 382, Contract Number 1866(32), Harvard University (1963).

4. R. W. P. King, R. B. Mack, and S. S. Sandler, *Arrays of Cylindrical Dipoles*, Chapter IV, Cambridge University Press (1968).

5. A. Grossmann and T. T. Wu, "A Class of Potentials with Extremely Narrow Resonances," *Chinese J. Phys.* **25**, 129–139 (1987).

HgTe/CdTe superlattices has been resolved [2]. We have shown that the effective mass and the band gap obtained in the magnetooptical experiments are consistent with the larger value of the valence band offset. This is due to the fact that the conduction and valence bands of the semiconductor superlattices cross as the offset is increased from small values and render the materials semimetallic. What had been missed is the fact that the superlattice again becomes semiconducting as the offset is increased further. This resolution of the dilemma is appealing because it recognizes that both magneto-optical and photoemission experimental results are consistent with each other and simply notes that there has been an oversight on the part of theorists in failing to recognize that after the semimetallic regime, the superlattice band structure becomes once again semiconducting with the band gap at the superlattice Brillouin zone. These results have been published in *Phys. Rev. Lett.* [1,2].

References:

1. N. F. Johnson, H. Ehrenreich and R. V. Jones, "Carrier-Activated Light Modulation," *Phys. Rev. Lett.* **53**(3), 180 (1988).

2. N. F. Johnson, P. M. Hui and H. Ehrenreich, "Valence Band Offset Controversy in HgTe/CdTe Superlattices: A Possible Resolution," *Phys. Rev. Lett.* **61**(17), 1993 (1988).

B. Magnetic Properties of Diluted Magnetic Semiconductors

The investigations of magnetic disorder in DMS have led to an empirically based and internally consistent picture of the electronic structure of these materials. This picture is consistent with the existing experimental information, and, to the best of our knowledge, inconsistent with none. It has been used to describe the magnetic interactions in the Mn-alloyed II-VI DMS on a microscopic basis. As a result, it has been possible to develop a description of the electronic and magnetic interactions on energy scales ranging from 10^{-5} eV to 10 eV.

We have considered compounds of the form $(II)_{1-x}Mn_x(VI)$ for a variety of ingredients belonging to Groups II (Hg,Cd,Zn) and VI (Te,Se,S) of the periodic table.

We have examined both isotropic and anisotropic exchange for CdMnTe and related materials. In the case of the isotropic exchange these represent the most accurate available results thus far for any magnetic insulator. The reason for this improvement is associated with better knowledge of the electronic structure for semiconductors and the utilization of the empirically determined Te p - Mn d exchange interactions.

During the past year we have published [1] a quantitative calculation of isotropic superexchange and an explanation of the spin resonance linewidth narrowing in diluted magnetic semiconductors. The Dzyaloshinski-Moriya anisotropic superexchange is the dominant mechanism determining the paramagnetic resonance (EPR) linewidth in Mn-based II-VI DMS such as $Cd_{1-x}Mn_xTe$. The Anderson Hamiltonian which was applied in our previous study of isotropic superexchange has been generalized to include the anion spin-orbit coupling responsible for anisotropic superexchange. The EPR lineshape has been calculated using a moment expansion of the magnetic response function to first order in inverse temperature together with a maximum entropy ansatz. The calculated infinite temperature linewidths are in good agreement with extrapolated experimental values obtained by Samarth and Furdyna. A novel fit of the theoretical temperature dependence to the experimental linewidth data provides the first empirical value for the anisotropic exchange constant. This value is in excellent agreement with that obtained by our theoretical calculation. The calculated chemical trends for the exchange constants for the selenides and sulfides yield the experimentally expected trends.

Reference:

1. B. E. Larson and H. Ehrenreich, "Anisotropic Exchange and EPR Linewidths in Diluted Magnetic Semiconductors", *Phys. Rev. B.* **39**(3), 1747 (1989).